COVARIANCE OF MICROFOSSIL ASSEMBLAGES AND MICROBIALITE TEXTURES ACROSS A LATE MESOPROTEROZOIC CARBONATE PLATFORM

ANDREW H. KNOLL[1,*], SARAH WÖRNDLE[2], and LINDA C. KAH[3]

[1]Department of Organismic and Evolutionary Biology, Harvard University, Cambridge MA 02138, USA, aknoll@oeb.harvard.edu; [2]Université Lyon-1 Claude Bernard, Département des Sciences de la Terre, 69622 Villeurbanne Cedex, France, sarah.worndle@hotmail.fr; [3]Department of Earth and Planetary Sciences, University of Tennessee, Knoxville, TN 37996-1410, USA, lckah@utk.edu

***** Corresponding author

RRH: *MICROFOSSILS AND MICROBIALITE FABRIC*

LRH: *KNOLL ET AL.*

Keywords: cyanobacteria, petrofabric, Baffin Island, Bylot Supergroup, taphonomy

ABSTRACT

Nodular and bedded cherts of the upper Mesoproterozoic Angmaat (formerly Society Cliffs) Formation, Baffin and Bylot islands, preserve microfossils and primary petrofabrics that record microbial mat deposition and lithification across a range of peritidal carbonate environments. Five distinct microfossil assemblages document the distribution of mat-building and mat-dwelling populations across a gradient from restricted, frequently exposed flats to more persistently subaqueous environments. Mats built primarily by thin filamentous or coccoidal cyanobacteria give way to a series of more robust forms that show increasing assemblage diversity with decreasing evidence of subaerial exposure. Distinct fabric elements are associated with each microbial assemblage, and aspects of these petrofabrics are recognizably preserved within unsilicified carbonates. These include some features that are distinctly geologic in nature (e.g., seafloor cements) and others that reflect microbial growth and decomposition (e.g., tufted microbialites). A particularly distinctive, micro-nodular fabric is here interpreted as carbonate infilling of primary voids within microbial mat structures. Such structures mark the confluence of cyanobacterial photosynthesis that produced oxygen gas, filamentous mat builders that imparted the coherence necessary to trap gas bubbles, elevated carbonate saturation required to preserve void fabrics via penecontemporaneous cementation, and a relative paucity of detrital sediment that would have inhibited mat growth. Petrofabrics preserved in Angmaat samples are widespread in late Paleoproterozoic and Mesoproterozoic carbonate successions but are rare thereafter, perhaps recording, at least in part, the declining carbonate saturation state of seawater. Covariation of microfossil assemblages with petrofabrics in both silicified and unsilicified carbonates supports hypotheses that link stromatolite microstructure to the composition and diversity of mat communities.

INTRODUCTION

Stromatolites constitute the most conspicuous record of life in Proterozoic sedimentary rocks. Stromatolites vary in morphology and fabric across individual basins and through time, but despite a century of research, there is little consensus on how this variation relates to microbial diversity (Grotzinger and Knoll, 1999). Aspects of stromatolite macrostructure clearly reflect sedimentary environment (Cloud and Semikhatov, 1969; Serebryakov, 1976; Semikhatov et al., 1979; Andres and Reid, 2006), but petrologic fabric may additionally preserve a record of distinct microbial communities and metabolic activities active during stromatolite accretion (Monty, 1976; Walter, 1992; Dupraz et al., 2006, 2009; Bosak et al., 2013). Testing biological hypotheses, however, is complicated by diagenesis, which can result in both the alteration of original petrofabrics and obliteration of the mat building populations in stromatolites. An exception occurs in the upper Mesoproterozoic Angmaat Formation, Bylot Supergroup, Nunavut, where early diagenetic chert nodules preserve both microbial mat populations and distinctive mat petrofabrics. Silicified fabrics, in turn, can be compared directly to textures preserved in associated unsilicified carbonates, allowing us to address specifically the question of how microbial community composition relates to mat fabric in selected Proterozoic carbonates.

GEOLOGIC SETTING AND AGE

The Bylot Supergroup comprises a >6 km-thick succession of nearly undeformed, late Mesoproterozoic to earliest Neoproterozoic sedimentary rocks exposed within the fault-bounded Borden Basin of northernmost Baffin and Bylot islands (Fig. 1., Jackson and Ianelli, 1981; Turner, 2009). Timing of sedimentation within the Bylot Supergroup is broadly constrained by U-Pb baddeleyite ages on basalts that both pre- and post-date sediment deposition. Basalts near

the base of the Bylot succession have yielded an age of 1270±4 Ga (Le Cheminant and Heaman, 1989), and Franklinian dykes that crosscut the supergroup as a whole record a maximum age of ~723 Ma (Heaman et al., 1992; Pehrsson and Buchan, 1999). Consistent with these constraints are a Pb-Pb age for Angmaat carbonates of 1199+/-24 Ma (unpublished data, in Kah et al., 2001) and a U-Th-Pb whole rock age of 1092+/-59 Ma for black shale of the underlying Arctic Bay Formation (Turner and Kamber, 2012). Carbon isotope stratigraphy independently suggests an age younger than ca. 1250 Ma and older than ca. 850 Ma (Kah et al., 1999, 2012), and microfossils suggest that the depositional age of Angmaat Formation strata lies closer to the lower than to the upper boundary established by regional basalts (Hofmann and Jackson, 1991, 1994). Micropaleontological data on correlative successions in northwestern Greenland (Strother et al., 1983; Samuelsson et al, 1999) and Somerset Island (Butterfield, 2001) further support a late Mesoproterozoic age for Angmaat deposition.

Sedimentary rocks of the Bylot Supergroup crop out extensively within the fault-bounded Borden Basin of northern Baffin and Bylot islands (Fig. 1; Jackson and Ianelli, 1981; Kah et al., 1999; Turner, 2009). Traditionally, deposition of a laterally extensive package of carbonate-dominated strata—originally distinguished as the Society Cliffs Formation—was considered to represent a period of relative tectonic quiescence within the basin, during which sea level rise promoted an extensive, northwestward deepening carbonate ramp (Blackadar, 1956; Lemon and Blackadar, 1963; Geldsetzer, 1973). Building on the work of Jackson and Ianelli (1981), who recognized a pronounced dimimution of siliciclastic material upward in the Society Cliffs Formation, and Kah (1997, 2000) and Kah et al. (1999, 2001), who recognized a distinct shift to deeper-water facies west of a persistent oolitic shoal in the region of Tremblay Sound, Turner (2009) divided the these strata into four formations (Iqqittuq, Angmaat, Nanisivik, and Ikpiarjuk)

that better reflect regional lithologic trends. Here we focus on the southeastern successions of the former Society Cliffs Formation, now considered the Angmaat Formation.

The Angmaat Formation records predominantly intertidal to supratidal carbonate deposition, with auxiliary siliciclastic, evaporite, and chert lithologies (Kah and Knoll, 1996; Kah et al., 2001). The majority of the Angmaat Formation represents *in situ* deposition within an evaporative microbial flat that was frequently restricted from open marine waters by subaerial exposure of a mid-ramp oolitic/intraclastic shoal complex (Kah, 1997; Kah, 2000; Kah et al., 2001). Inner ramp carbonate facies are dominated by microbialite facies, with subordinate precipitate facies, and rare detrital lithologies.

Microbialites comprise a variety of low relief stratiform, domal, columnar, and coniform structures. Coniform stromatolites with distinct concave upward laminae form interlinked features up to 20 cm in synoptic relief, and are restricted to deepest-water portions of the Angmaat platform, where they are interbedded with columnar stromatolites and oolitic/intraclastic shoal facies. In the inner ramp, coniform microbialites are restricted to mm- to cm- scale tufted mats (see below) that interfinger laterally with the more abundant smooth and micro-nodular laminae that comprise the majority of stratiform mat facies. Tufted laminae, however, are more common in restricted portions of the ramp, where they are interlaminated with precipitated carbonate facies, often in the construction of broad, domal features.

Precipitate facies consist of smooth sub-millimeter laminae in which discrete laminations can often be traced 10's to 100's of meters of outcrop exposure and reflect a continuum of nucleation patterns. Continuous nucleation along the substrate, results in laterally extensive isopachous crusts; isolated nucleation sites result in the formation of small (generally <5 mm) cement botryoids on bedding surfaces. Successive lamina growth atop these smooth to bumpy

surfaces resulted in formation of a range of precipitate forms from hemispherical domes to microdigitate, or asperiform, structures (c.f., Hofmann & Jackson, 1986).

Detrital carbonate facies are rare within the Angmaat Formation, and consist primarily of thin micritic drapes, local arenites, and a variety of intraclastic conglomerates deposited under higher-energy, less restricted conditions. Evaporite lithologies—predominantly gypsum—are broadly distributed within the Angmaat Formation (Kah et al., 2001), but are relatively rare in the Milne Inlet Trough, where they occur only as cm-scale nodules within stratiform mats and within a few discrete beds (up to 1.45 meters thick; Kah et al., 2001). Within the Milne Inlet trough, bedded gypsum occurs primarily in the southeast, where it is intimately associated with precipitate facies and thin beds of terrigenous red to green shale.

Finally, the Angmaat Formation (and correlative strata in adjacent grabens in northwestern Greenland and on Somerset Island; Kah et al., 1999) contains abundant nodular to bedded chert (Jackson and Ianelli, 1981). Cherts display a wide range of colors, from white to grey, yellow to orange, green to purple, and brown to black, and occur in variously shaped bodies that are commonly discordant to bedding (Jackson and Ianelli, 1981; Hofmann and Jackson, 2001). Black chert is most abundant, especially in the region between Milne Inlet and Tay Sound (Fig. 1), forming beds and nodules oriented parallel to bedding and up to 10 cm in thickness. Black cherts typically preserve microfossils (Hoffman and Jackson, 2001; Kah and Knoll, 1996; see also Strother et al., 1983,and Butterfield, 2001, for fossiliferous cherts from coeval strata in adjacent grabens), although more poorly preserved microfossils have been found in a wide variety of colored chert (Hoffman and Jackson, 2001).

MICROFOSSILS IN ANGMAAT MICROBIALITES

Attempts to evaluate the relationship between microbial community and microbialite petrofabric begin with the elucidation of preserved microfossil assemblages. Hofmann and Jackson (1991) described silicified microfossils from throughout the (then) Society Cliffs and overlying Arctic Bay formations. Their most diverse fossil localities occur in the Arctic Bay succession and there was no attempt to relate fossils to petrofabric. Nonetheless, most of the taxa found in our Angmaat chert samples were noted by Hofmann and Jackson (1991).

Most mat building populations in Angmaat microbialites are preserved as hollow filamentous tubes—the preserved extracellular polysaccharide sheaths of *Lyngbya*- or *Phormidium*-type cyanobacteria (Figs. 2-4). By convention, single sheaths are assigned to the genus *Siphonophycus* Schopf (1968) and divided into species based on cross-sectional diameter. Remarkably, most Proterozoic *Siphonophycus* populations fit comfortably within one of these operationally defined species (e.g., Knoll et al., 1991). Hofmann and Jackson (1991) recognized the three species-level *Siphonophycus* taxa noted in our study, although the population here assigned to *S. capitaneum* on the basis of size was placed into the smaller *S. kestron* by these authors. They also named several small and poorly preserved taxa, which we view as degradational variants of the principal mat-building filaments.

Distinctly larger (up to 70 μm in cross-sectional diameter) filamentous sheaths (Fig. 3D) that originally enclosed multiple cellular trichomes (see cross-section in Fig. 3E) are assigned to *Eomicrocoleus crassus* Horodyski and Donaldson (1980) and interpreted in terms of the extant mat-building cyanobacterium *Microcoleus chthonoplastes.* (Note that when the microscope is ratcheted up and down through *E. crassus* specimens, the internal reflections of trichomes—seen

as lineations in Fig. 3D—can be shown to form a rope-like coiling that, in the modern, is a diagnostic feature of *M. chthonoplastes*; Desikachary, 1958).

Microfossils in Angmaat cherts also include abundant and diverse coccoidal populations, many, if not most of them, cyanobacterial (Figs. 4-6). Early in the modern era of Proterozoic paleontology, spheroid-rich assemblages were discovered on several continents and assigned to a large number of narrowly diagnosed taxa; Butterfield (2001) summarized the resulting challenges for taxonomy. Whereas some of the complications simply reflect synonomy, others stem from aspects of life cycle and taphonomy (e.g., Knoll and Golubic, 1979), offering a principled path toward resolution. Sorting out all issues of Proterozoic microfossils taxonomy is beyond the scope of this paper, but we can propose distinctions among the main mat-forming populations present in Angmaat cherts.

Populations of small, mat-building coccoidal colonies are assigned to *Eoentophysalis belcherensis* Hofmann (1976) and interpreted in terms of the extant mat-building genus *Entophysalis*. Small (2-5 μm) cell-like units are bound into colonies by extracellular envelopes secreted with each new cell division; resulting clusters contain 2-32 cells within up to five nested envelopes. Colonies are palmelloid to cumulate (Fig. 4B), but also include isolated unicells, dyads and smaller clusters, many of which were described as separate species in early papers (e.g., Muir, 1976). A principal problem with the taxonomic circumscription of *Eoentophysalis* is that new colonies begin with individual cells, so colonizing eoentophysalids may be difficult or impossible to differentiate from similarly small, non-colonial taxa such as *Sphaerophycus parvum* Schopf (1968). *Sphaerophycus* populations are not always eoentophysalid colonists, as many *S. parvum* (Fig. 4D,E; ca. 2 μm cell-like units) and (slightly larger; 4-5 μm units) *S. medium* Hofmann and Donaldson (1980; Fig. 5C,D) populations occur in facies where

eoentophysalid colonies are absent, both in the Angmaat and in other formations. Populations of small coccoids could include heterotrophic bacteria. Erring on the side of caution, we recognize *Sphaerophycus* populations only when isolated unicells, dyads and tetrads are distributed through mats in the absence of reasonably well-formed *Eoentophysalis* colonies.

Like Hofmann and Jackson (1991), we also recognize two species of the cyanobacterial form genus *Gloeodiniopsis* Schopf (1968) emend. Knoll and Golubic (1979). *Gloeodiniopsis lamellosa* is applied to populations of multilamellate (or single envelope, by differential decay) unicells, dyads, tetrads, and rare octads, distributed as isolated individuals in eoentophysalid and filamentous mats but never found in dense colonies (Fig. 4I-L). The simple life cycle and taphonomic pattern inferred for these populations compares closely with those of the extant cyanobacterium *Chroococcus turgidus* (Knoll and Golubic, 1979). A second *Gloeodiniopsis* species, *G. magna* Nyberg and Schopf (1984), is spatially distinct and much larger, but shares the basic life cycle inferred for *G. lamellosa* (Fig. 4G,5E).

Eogloeocapsa bella Golovenok and Belova (1984) can be difficult to differentiate, given its high degree of taphonomic variation, but well-preserved populations document a life cycle comparable to that observed in extant species of *Gloeocapsa* (Geitler, 1930-1932). *Eogloeocapsa* thus differs from *Gloeodiniopsis* in three principal ways: internal envelopes formed around a single cell fill a smaller percentage of the volume formed by enclosing envelopes (that is, cell-like internal envelopes are not close-packed but rather appear to "float"); there is a single external envelope, unlike the multilamellate exterior of *Gloeodiniopsis*; and colonies can be closely packed to form mono-specific surfaces in peritidal environments (Fig. 6A-C). As discussed by Sergeev (1994), there is some potential for confusion in terms of another Proterozoic taxon *Clonophycus elegans* Oehler (1977), but the type of *C. elegans* is an outer

envelope filled by a large number of closely packed cells, with no evidence of intermediate envelopes. This differs substantially from both the type of *E. bella* and the Angmaat material.

Polybessurus bipartitus Fairchild ex Green et al. (1988) is a coccoidal cyanobacterium distinguished by its prominent stalk formed by downwardly elongated envelopes (Fig. 5A,B). In terms of morphology, life cycle and environmental preference, these fossils find a close counterpart in *Cyanostylon*-like cyanobacteria from peritidal carbonate environments in the present day Bahamas (Green et al., 1987).

At least two additional populations of simple spheroids occur in filamentous mats, one 8-10 μm (Fig. 5F) and the other 25-30 μm in diameter (Fig. 3F). These populations are readily placed within the form genus *Myxococcoides* Schopf (1968), and might be assigned to *M. minor* Schopf (1968) and *M. grandis* Horodyski and Donaldson (1980) on the basis of size, but the Angmaat populations are sufficiently different from the types of these species to urge caution. For this reason, we refer to them simply as *Myxococcoides* sp. 1 and sp. 2. Two more unnamed populations consist of poorly preserved, *Hyella*-like endolithic cyanobacteria, interpreted on the basis of overall morphology and orientation – which clearly indicates downward growth into the substrate (Fig. 4A), and clustered unicells ca. 25 μm in diameter from which 10-12 μm tubes extend outward for up to 50 μm (Fig. 4H). The latter fossils appear to be germinating cysts, like the Neoproterozoic *Germinosphaera* (see Butterfield et al., 1994, for interpretation) but at a much smaller size scale. Multilamellate unicells that appear to open on one end (Fig. 4F; also documented by Butterfield, 2000, from the correlative Hunting Formation on Somerset Island) may be an incipient excystment stage of the same population.

The final constituents of our Angmaat samples are isolated cellular filaments found within *E. robustum* mats. These fossils can be assigned to the early red alga *Bangiomorpha*

pubsecens Butterfield (2000), described from potentially correlative strata (Kah et al., 1999) on Somerset Island and, possibly, northwestern Greenland (Enzien, 1990). Angmaat specimens (Fig. 6D,E) observed to date do little to augment the paleobiological interpretation of this taxon, adding only that the envelopes surrounding cellular filaments can form septa that separate packets of a dozen or more cells. When preserved in the absence of cells, these would be closely comparable to the unnamed septate tubes described by Butterfeld (2000, his Fig. 3E) from *Bangiomorpha*-bearing beds on Somerset Island.

CORRELATING MICROFOSSILS AND PETROFABRIC

Crystal fan-dominated precipitates

Flat laminated and domal carbonates, interpreted as originally aragonitic seafloor precipitates, are conspicuous features of Angmaat outcrops (Kah et al., 2001; Turner, 2009). Where preserved as dolomite, precipitated laminae consist of mm-scale laminations with mm- to cm-scale, convex-upward microdomal surfaces (Fig. 7A). Laminae consist, for the most part, of interlocking dolomite anhedra up to ca. 80 μm in maximum dimension capped by thin drapes of dolomitic microspar that commonly preserve ghosts of upward-directed crystal terminations. Even in these relatively coarse-grained dolostones, UV fluorescence highlights organic inclusions that define acicular needles and sprays of crystalline carbonate that grew perpendicular to the substrate. Minute pyrite crystals (or iron oxides formed by diagenetic pyrite oxidation) are common within microspar laminae (black minerals in Figs. 7B,C,F). Dolospar laminae also have irregular clear patches that impart a clotted microtexture to the carbonates.

Early diagenetic chert further clarifies the origin of textures observed in encompassing carbonates. The principal fabric elements are mm-scale crystal fans, originally deposited as seafloor carbonate precipitates. The majority of precipitate textures consist of acicular crystals up to 2 mm long but no more than a few μm thick (Fig. 7B, C). In some places, however, thicker (ca. 30 μm) crystals show square terminations indicative of original aragonite (Fig. 7E). Discontinuous mm-scale lamination, visible to the naked eye, is resolved in thin section as zoned precipitates, pigmented more or less strongly by included organic matter (Fig. 7A, F). Similar precipitates form today in local environments of extreme oversaturation, for example, calcitic precipitates formed in leachate pipe systems in Florida (Maliva et al., 2000). More continuous surfaces show a granular texture, with relatively abundant 1-5 μm pyrite crystals; these are interpreted as exposure surfaces that underwent micritization prior to silica emplacement. Light patches in the chert are largely irregular dissolution features, now filled by silica and dolomite euhedra, and often surfaced by tiny pyrite crystals (Figs. 7B,C).

Fabric elements preserved in chert map fairly straightforwardly onto textures apparent in unsilicified carbonates of this facies. The mm-scale laminations so prominent in unsilicified carbonates correspond to the micritized exposure surfaces observed in the chert (Fig. 7A). Crystal fans, well preserved in chert, have been recrystallized completely to dolospar in carbonate phases, with dissolution features preserved as clear irregular patches within dolospar layers. Microfossils are rare in this facies—the only possible candidate fossils are isolated, hollow organic filamentous structures oriented parallel to the long axes of crystals that could be the remains of endolithic cyanobacteria (Fig. 7D).

Thin-Filament Tufted Mat

In outcrop, vertically-striped black and white chert is commonly associated with cm-scale tufted microbialites (Fig. 8), and interbedded with precipitate textures. Tufts are interpreted to reflect synsedimentary cementation that conferred structural rigidity onto vertical tufts of cyanobacterial filaments; and cherts similarly reflect interaction of microbial behavior elements and synsedimentary cement. In thin section, the black regions of variegated chert nodules are resolved as dense populations of thin filaments and associated biofilm; the white regions are cemented-filled voids (Fig. 9).

Microfossils in this facies comprise a single population of thin cylindrical filaments (Fig. 9B,C). Most filaments show evidence of partial decay and collapse, yielding micron-thick, commonly fragmented individuals. In well-preserved regions, filaments are preserved as 2-3 μm hollow, filamentous tubes ascribed to *Siphonophycus robustum* (Schopf) Knoll et al. (1991) and interpreted as the extracellular sheaths of *Phormidium*-like cyanobacteria. The spatial orientation of *S. robustum* populations is distinctive: vertical bundles of filaments form tent-pole structures from which sheets of filaments extend outward and attach to adjacent vertical elements, forming convex downward laminae that isolated primary void space (Fig 9B,C). Voids are generally subrounded and commonly contain silicified splays of acicular carbonate that formed prior to silicification (arrow in Fig. 9C). The voids closely resemble gas bubbles trapped in modern mats (Bosak et al., 2010; Mata et al., 2012). Some samples also contain mm- to cm-scale voids that crosscut mat fabrics and are interpreted as dissolution features. Void structures within tufted thin-filament mats were filled during diagenesis by an isopachous lining of chalcedony and, in their centers, by large twinned dolomite crystals. Within Angmaat cherts, gas bubbles and dissolution features are readily distinguished, but in associated carbonates, differentiation of these structures is more difficult.

The fabric of the thin-filament tufted mats resembles that described by Sumner (1997) from cuspate stromatolites in the 2.52 Ga Gamohaan and Frisco formations, South Africa. Microfossils are not preserved in the Archean examples, but preserved petrofabrics suggest that filamentous microorganisms formed vertical supports that were cemented penecontemporaneously with mat growth. Perhaps slightly flocculent mats draped across the vertical supports, forming highly porous constructions filled by synsedimentary cement. The spatial scale of the Archean structures is much larger—cm- to m-scale cusps as opposed to the mm-scale features observed in Angmaat cherts—although similar but larger coniform structures are preserved in deeper-water facies of the Angmaat Formation. Archean coniform structures similarly formed at depth during the drowning of an extensive carbonate platform—a setting far different from the peritidal environments discussed here. Nonetheless, the two examples appear to reflect common processes of population growth and penecontemporaneous cementation.

The thin section illustrated in Fig. 9A shows that where these mats were not silicified, compaction commonly resulted in an irregular fabric whose origin would be difficult to interpret in the absence of chert preservation: the fabric is dominated by dark stringers interpreted as compacted mats and lighter clots interpreted as void-filling precipitates. A thin layer at the base of the thin section composed of uniform, isopachous cements indicates that seafloor precipitates and thin filament tufted mats formed in close environmental proximity.

Laminated Precipitates and Coccoid-Rich Mats

Stratiform laminites occur in carbonate successions through the Proterozoic record and are usually interpreted as flat mats that trapped and bound or precipitated carbonate sediments. Consistent with this larger record, stratiform laminites are common in the Angmaat succession.

In carbonates, these consist of subtly undulating mm-scale microspar laminae, with finer-grained, and hence darker, microspar defining lamina surfaces (Fig. 10A). Silicified samples present a more nuanced picture of this facies, with mat layers (Fig. 10B) interlaminated with a combination of finely laminated precipitate structures (Fig. 10C) and fine intraclastic microbreccias. The mat layers commonly contain undulating to billowy organic matter; with denser organic accumulations corresponding to the dark microspar surfaces observed in associated carbonates. Early diagenetic pyrite is common, especially in organic rich laminae, but microfossil preservation is typically poor. Precipitate layers up to about 300 μm thick consist of 5-10 μm layers defined by slight organic pigmentation along their surfaces. In carbonate, it is impossible to tell which laminae formed as mats and which originated as precipitate horizons. Intraclastic microbreccias are locally common in this facies, and are associated with cement-filled voids formed by dissolution. These features are recorded in non-silicified facies as detrital layers and sparry patches, both visible in thin section (Fig. 10A).

Where microfossils are preserved, microbial populations are almost exclusively coccoidal, with *Eoentophysalis belcherensis* Hofmann (1976) as the dominant builder (Fig. 4B) and *Gloeodiniopsis* species locally abundant as mat dwellers (Fig. 4I-L). The association between laminated precipitates and entophysalid cyanobacteria has been noted previously, both in the Angmaat Formation and elsewhere (Knoll and Sergeev, 1995; Sergeev et al. 1995; Kah and Knoll, 1996). Either coccoid populations were favored on the substrate provided by seafloor precipitates, or filamentous populations were inhibited. Locally, this facies also contains rare isolated individuals of the stalked cyanobacterium *Polybessurus* (Fig. 5A,B) and endolithic cyanobacteria (Fig. 4A). Within a single thin section, stratiform precipitates and coccoid mats can be interbedded with mats formed by fine filamentous cyanobacteria that trapped gas bubbles

preserved as cement-filled primary void space (Fig. 11). Thus, these two biofacies/microfabrics must have been contiguous on the Angmaat platform.

Filament-Dominated Mats

Two distinct filamentous mat assemblages can be differentiated within Angmaat cherts. The first, interlaminated with the stratiform precipitates and *Eoentophysalis* mats described in the previous section (Fig. 11A), consists of thin (2-3 μm cross-sectional diameter) filamentous sheaths assigned to *Siphonophycus robustum* (Figs. 4C). The filaments are commonly oriented vertically and are associated with abundant extracellular polymeric substances, or EPS; coccoidal cyanobacteria occur among filaments in the mat assemblage as do the stalk-forming cyanobacterium *Polybessurus* and the filamentous red alga *Bangiomorpha* Butterfield (2000). Filaments commonly line primary, mm-scale globular voids filled by early diagenetic cement; most of the voids appear to have formed as gas bubbles preserved by penecontemporaneous calcification of entrapping filaments. In some cases, voids remain wholly or partially filled by early microspar cement (Fig. 11A); evidently these cements occluded porosity, limiting the subsequent incursion of silicifying fluids. Microspar fill is also conspicuous in surrounding carbonates, forming irregular clots lined by highly compacted, commonly organic-darkened mat dolomicrite (lower part of Fig. 11A).

A much different filament assemblage occurs in thicker (mm-scale lamination) undulating (and less frequently tufted) mats that only occasionally preserve primary void spaces (Fig. 12). The primary mat builder in these mats is *Siphonophycus inornatum* Zhang (1981), ca. 6 μm filaments that form densely interwoven populations (Fig. 3A). A subset of these mats also contains thicker (up to 25 μm cross-sectional diameter) and more deeply pigmented sheaths

assigned to *Siphonophycus capitaneum* Nyberg and Schopf (1984) (Figs. 2,3C), and a smaller subset also contains much larger sheaths that contained multiple trichomes, assigned to *Eomicrocoleus crassus* Horodyski and Donaldson (1980) (Fig. 3D,E). On the scale of individual thin sections, assemblage composition (1, 2 or 3 filamentous taxa) appears to be consistent within individual laminae, but varies vertically from one layer to the next. Filament orientation also varies from one lamina to another; populations can be oriented horizontally or vertically, and commonly alternate repeatedly within a single thin section. Vertically-oriented filaments occasionally result in cm-scale tufts with substantial void space (Fig. 12B). Thick silicified mats without trapped bubbles or dissolution features invariably contain predominantly horizontally-oriented laminae of these three mat-building filaments.

Co-occurring, but numerically subordinate coccoidal populations include *Gloeodiniopsis*, *Polybessurus, Sphaerophycus medium* Horodyski and Donaldson (1981), the simple spheroids assigned to two species of *Myxococcoides,* and unnamed coccoidal microfossils from which elongate tubes emerge (Figs. 3F,4H,5F). Less commonly, *S. inornatum* mats also contain isolated clusters of *Eogloeocapsa* . Fossil preservation is variable through these mats; laminated EPS with few or no discrete microfossils intergrades with expanded mats containing exceptionally well preserved microfossils. In all cases, the dark *S. capitaneum* sheaths preserve differentially well. This differential preservation can be observed, as well, in associated unsilicified carbonates, where mat fabrics comprised of vertically oriented filaments of *S. capitaneum* are occasionally preserved via *in situ* mineralization of filament sheaths (Fig. 2E; see also Kah and Riding, 2007).

Modern microbial mats at Laguna Mormona, in Baja California (Horodyski et al., 1977), provide a useful framework for interpreting filamentous microbialites in the Angmaat

succession. Microbial mats within peritidal environments at Laguna Mormona have undulating 1-3 mm laminae similar to those in Angmaat cherts (Fig. 5 in Horodyski et al., 1977) built by a community of filamentous cyanobacteria that includes large *Microcoleus chthonoplastes, Lyngbya aestuarii* (with 20-25 μm sheaths), and smaller filamentous populations. Similar to the Angmaat assemblage, the sheaths of *L. aestuarii* preserve differentially well at Laguna Mormona and become the most apparent taxon at depth within the mats, regardless of their proportional abundance in surface communities. And, as in the Angmaat Formation, filamentous mats at Laguna Mormona occur in close spatial proximity to *Entophysalis* mats that (1) are associated with local seafloor aragonite precipitation and (2) have a relatively low preservation potential (Horodyski and vonder Haar, 1975).

Eogloeocapsa-rich Laminae

Within thin sections of flat- laminated filamentous mats, a few laminae are texturally and paleobiologically distinct. These layers commonly contain poorly preserved *Eoentophysalis* populations, but they are dominated by large colonial coccoids assigned to *Eogloeocapsa bella* Golovenok and Belova (1984) (Fig. 6A-C,13) and interpreted in terms of the extant cyanobacterial genus *Gloeocapsa*. *Eogloeocapsa*-rich laminae differ from filamentous mat layers in the same thin section by their cumulate texture and an absence of internal lamination (Fig. 13). Although clearly distinguished in chert nodules, filamentous and *Eogloeocapsa*-rich layers are difficult to tell apart in associated carbonates.

DISCUSSION

Microbes and Microbialites along the Angmaat Platform

Petrographic variations suggest that the principal petrofabrics identified in Angmaat cherts can be ordered along a gradient of decreasing environmental restriction and subaerial exposure, identified on the basis of variations in seafloor carbonate precipitates and evidence for post-depositional dissolution (Fig. 14). This ordering may be simplistic, as petrofabric generation might easily vary along axes other than water depth, but it finds support in the distribution of microfossil populations within the formation. Restricted facies with abundant evidence for subaerial exposure also have the lowest diversity of microfossils, whereas petrofabrics interpreted as less frequently exposed (or, more persistently wet) harbor a larger number of taxa. Many taxa occur in more than one petrofabric, and when placed in the spatial order suggested by petrofabric, all but one show contiguous distributions (Fig. 14). Kah and Knoll (1996) also noted that the number of chert samples represented by the main fabric types varied spatially within the basin, again indicating a broad-scale covariance between microfossil assemblages and depositional texture in the Angmaat cherts. To a first approximation, then, microfossil assemblages map one-to-one onto preserved depositional textures, supporting the hypothesis that microbialite petrofabric reflects, at least in part, microbial community composition.

Microbial populations influence petrofabric development in a number of ways. Mat-building populations can trap and bind fine particulate carbonate, leading to stromatolite accretion when accompanied by cementation. Microbially-induced precipitation can also govern carbonate accumulation in the absence of trapping and binding, and this appears to be the case in our Angmaat samples (Kah and Knoll, 1996). More specific features of microbial populations can also influence petrofabric: did the organisms produce extracellular sheaths or envelopes that resist decay and act as nucleation sites for carbonate precipitation? Were filament populations oriented vertically or horizontally, a reflection of microbial behavior that influences the spatial

pattern of precipitation? Did mats have sufficient cohesion to trap gas bubbles and retain them until precipitation occurred?

Of course, physical setting will also influence petrofabric by governing the degree of carbonate oversaturation, imposing shear stress on mat communities, and introducing traction or suspension-load sediment particles. In most stromatolites, observed petrofabric will reflect both both biological and physical processes, as well as later diagenesis. The Angmaat microbialites are exceptional in that early diagenetic chert allows us to distinguish primary fabrics formed by interacting biological and physical processes from the more common petrofabrics that additionally reflect carbonate diagenesis.

The principal fabric elements in the Angmaat samples include tabular to acicular seafloor precipitates, fine-grained precipitated carbonates that preserve filament orientation, cement-filled primary void space generated by gas bubbles, and cement-filled secondary void space produced by dissolution. Clastic microbreccias occur in association with precipitate-rich laminae, and thin sandstones occur locally beneath some of the most diverse mats (Fig. 12A); detrital carbonate, however, appears to have played little role in Angmaat microbialite accretion.

The Stratigraphic Distribution of Angmaat Petrofrabrics

Primary voids preserved in Angmaat samples are particularly interesting because comparable petrofabrics are relatively abundant in Mesoproterozoic carbonate rocks (Fig. 15A-C). The formation and preservation of these voids require a source of biogenic gas (Bosak et al., 2010), a mat sufficiently cohesive to trap gas bubbles (Mata et al., 2012), carbonate precipitation on a time scale sufficiently rapid to frame the voids before elimination by compaction or

diffusion, and an absence of traction- or suspended-load sedimentation that would compromise mat development, bubble formation and retention, and rapid cementation.

As pointed out by Bosak et al. (2010), oxygenic photosynthesis is the only form of photoautotrophy that produces gas (O_2) as a by-product. The presence of at least moderately oxidizing surface environments in the Mesoproterozoic Era (Kah and Bartley, 2011) makes it likely that cyanobacteria dominated primary production in Angmaat mat communities, and beautifully preserved cyanobacterial fossils corroborate the view that gas bubbles likely originated via oxygenic photosynthesis. Within the Angmaat setting, only filament-dominated mats (and mixed filamentous-coccoid mats) contain primary void fabrics, suggesting that mat communities lacking filamentous populations populations may not have had the structural coherence required to trap and retain gas bubbles.

Microbial mats dominated by filamentous cyanobacteria occur commonly in Neoproterozoic successions that lack preserved bubble textures (e.g., Knoll et al., 1991; Cao and Yin, 2011). Thus, the additional key to primary void preservation must lie in penecontemporaneous mineral precipitation. As found in other Paleo- and Mesoproterozoic carbonate successions (Knoll and Semikhatov, 1988; Bartley et al., 2000; Grotzinger and James, 2000; Kah et al., 2012), (originally) aragonitic crystal fans indicate that the Angmaat basin was at least episodically restricted to the point at which carbonate readily nucleated in or on the shallow seafloor.

Preservation of primary void textures requires that thin mats buoyed by oxygen bubbles also acted as nucleation sites for carbonate precipitation. Local carbonate nucleation could reflect high abundances of Ca^{2+} absorbed onto cyanobacterial sheaths and biofilm polymers (e.g., Pentecost and Riding, 1986; Dupraz et al., 2009). OH^- generated by carbon dioxide

concentrating mechanisms in cyanobacteria might also have facilitated carbonate precipitation, as it does in some modern freshwater environments (Merz, 1992; Kah and Riding, 2007). Microbial sulfate reduction has also been linked empirically to carbonate precipitation within mats; whether dissimilatory sulfate reduction increases or decreases the probability of carbonate precipitation depends on substrate being metabolized (Gallagher et al., 2012) and the fate of H_2S generated by this process (Canfield and Farquhar, 2009). Under favorable circumstances, the net result is an increase in pH, facilitating carbonate precipitation (Aloisi, 2008). Microbial iron reduction provides another heterotrophic metabolism that would increase carbonate oversaturation within mats (Fischer and Knoll, 2009). Thus, within Proterozoic mat communities, a variety of microbial processes could have contributed to penecontemporaneous carbonate cementation (Aloisi, 2008).

That seafloor carbonate precipitates and preserved gas bubble textures are widespread in peritidal microbialites of late Paleoproterozoic and Mesoproterozoic age (Fig. 15), but uncommon in younger Neoproterozoic successions (e.g., Knoll and Swett, 1990) prompts the question of what was different in younger coastal environments. Filamentous cyanobacteria and anaerobic bacterial metabolisms didn't go away, suggesting that the most likely shift was in the carbonate saturation state of seawater. This has previously been proposed as a principal driver of secular change in Proterozoic stromatolite morphology (Grotzinger and Knoll, 1999) and changes in the distribution of abiotic carbonate fabrics, such as seafloor precipitates (Kah and Knoll, 1996) and 'molar-tooth' microspar (Pollock et al., 2006), and it has also been used to explain fundamental shifts in the marine C-isotope record (Bartley and Kah, 2004). What governed such changes, however, has proven elusive. Declining $[CO_3^{2-}]$ is consistent with a Neoproterozoic expansion in gypsum and anhydrite deposition (Kah et al., 2001), and might

reflect a general decrease in DIC associated with high rates of organic carbon burial, inferred from carbonate C isotopic abundances (Knoll et al., 1986; Bartley and Kah, 2004; Halverson et al., 2005). Whatever the causation, the sedimentary record indicates that carbonate fabrics like those in the Angmaat succession, which record precipitation mostly on and within benthic mats and the shallow substrate, were replaced in part by carbonate fabrics that refect a greater abundance of material precipitated as whitings from the water column (Kah and Knoll, 1996), largely restricting the petrofabrics described here to older successions.

Microbialite Fabric Preservation in Angmaat Carbonates

As described earlier in this paper, microbialite fabrics in Angmaat carbonates can be interpreted in light of biological and physical processes inferred from early diagenetic cherts. With the exception of filament cast and molds, direct fossil evidence of mat-building communities is not preserved in unsilicified Angmaat carbonates. Nonetheless, digenesis has not obliterated fabrics associated with seafloor precipitates, tufts formed by locally vertical filament growth, trapping of gas bubbles by filamentous mat populations, and undulating mats built by filamentous cyanobacteria. That is, diagenesis has operated on a template provided by depositional fabrics, and so microbialite textures preserved in carbonate facies do reflect microbial mat composition, at least in part. As noted above, biological inferences drawn from Angmaat petrology owe much to the physical circumstances of their formation, namely, penecontemporaneous carbonate precipitation from highly oversaturated waters. More generally, however, under favorable circumstances, petrographic textures imparted by trapping and binding, coccoidal vs. filamentous mat construction, filament orientation, and mat builder diversity may all leave a petrographic

signature in Proterozoic stromatolites (see also Walter et al., 1988; Knoll and Semikhatov, 1998; and references therein).

CONCLUSION

Silicified carbonates in the late Mesoproterozoic Angmaat Formation preserve depositional fabrics that are widespread in Paleoproterozoic and Mesoproterozoic carbonate rocks but uncommon in Neoproterozoic successions. Abundant microfossil populations preserved in these same cherts indicate that the biological composition of mat communities covaried in space with the preserved petrofabrics. Later diagenesis in unsilicified carbonate rocks altered but did not erase mat-specific petrofabrics. Thus, despite the obfuscating influence of carbonate diagenesis, the Angmaat samples support the hypothesis that microstructural fabrics in Proterozoic stromatolites can provide a tractable record of community diversity in ancient mat ecosystems.

ACKNOWLEDGEMENTS

We thank two anonymous reviewers for helpful criticisms of our original manuscript. Field work was supported by National Geographic Society Grant 5304-94 (to LCK) and logistical support from the Polar Continental Shelf Project. AHK acknowledges support from the NASA Astrobiological Institute. SW thanks Professor Fabrice Cordey for supporting her internship at Harvard.

REFERENCES

ANDRES, M.S., and REID, R.P., 2006, Growth morphologies of modern marine stromatolites: a case study from Highborne Cay, Bahamas: Sedimentary Geology, v. 185, p. 319-328, doi: 10.1016/j.sedgeo.2005.12.020.

BARTLEY, J.K., 1996, Actualistic taphonomy of Cyanobacteria: implications for the Precambrian fossil record: Palaios, v. 11**,** p. 571-586, doi: 10.2307/3515192.

BARTLEY, J.K., and KAH, L.C., 2004, Marine carbon reservoir, C_{org}-C_{carb} coupling, and the evolution of the Proterozoic carbon cycle: Geology, v. 32, p. 129-132, doi: 10.1130/G19939.1.

BARTLEY, J.K., KNOLL, A.H., GROTZINGER, J.P., and SERGEEV, V.N., 2000, Timing of early marine lithification and stromatolite biogenicity in peritidal silicified carbonates of the Mesoproterozoic Billyakh Group, Siberia: SEPM Special Publication, n. 67, p. 59-73.

BLACKADAR, R.G., 1956, Geological reconnaissance of Admirality Inlet, Baffin Island, Arctic Archipelago, Northwest Territories. Geological Society of Canada, Paper 55-6.

BOSAK, T., BUSH, J., FLYNN, M., LIANG, B., Ono, S., Petroff, A. P., and Sim, M. S., 2010, Formation and stability of oxygen-rich bubbles that shape photosynthetic mats: Geobiology, v. 8, p. 45-55, doi: 10.1111/j.1472-4669.2009.00227.x.

BOSAK, T., KNOLL, A.H., and PETROFF, A.P., 2013, The meaning of stromatolites: Annual Review of Earth and Planetary Sciences, v. 41, p. xxx-xxx, doi: 10.1146/annurev-earth-042711-105327.

BUTTEFIELD, N.J., 2000, *Bangiomorpha pubescens* n. gen., n. sp.: implications for the evolution of sex, multicellularity and the Mesoproterozoic/Neoproterozoic radiation of eukaryotes:

Paleobiology, v. 26, p. 386-404, doi: 10.1666/0094-8373(2000)026<0386:BPNGNS>2.0.CO;2.

BUTTERFIELD, N.J., 2001, Paleobiology of the late Mesoproterozoic (ca. 1200 Ma) Hunting Formation, Somerset Island, Arctic Canada: Precambrian Research, v. 111, p. 235-256, doi: 10.1016/S0301-9268(01)00162-0.

BUTTERFIELD, N.J., KNOLL, A.H., and SWETT, K., 1994, Paleobiology of the Neoproterozoic Svanbergfjellet Formation, Spitsbergen: Fossils and Strata, v. 34, p. 1-84.

CANFIELD, D.E., and FARQUHAR, J., 2009, Animal evolution, bioturbation, and the sulfate concentration of the oceans: Proceedings of the National Academy of Sciences, USA, v. 106, p. 8123-8127, doi: 10.1073/pnas.0902037106.

CAO, R., and YIN, L., 2011, Microbiota and microbial mats within ancient stromatolites in South China: Cellular Life, Life in Extreme Environments and Astrobiology, v. 18, p. 65-86.

CLOUD, P.E., and SEMIKHATOV, M.A., 1969, Proterozoic stromatolite zonation: American Journal of Science, v. 267, p. 1017-1061.

DESIKACHARY, T.V., 1959, Cyanophyta: Indian Council of Agricultural Research, New Delhi, 686 p.

DUPRAZ, C., PATTISINA, R., and VERRECCHIA, E.P., 2006, Translation of energy into morphology: simulation of stromatolite morphospace using a stochastic model: Sedimentary Geology, v. 185, p. 185-203, doi: 10.1016/j.sedgeo.2005.12.012.

DUPRAZ, C., REID, R.P., BRAISSANT, O., DECHO, A.W., NORMAN, R.S., and VISSCHER, P.T., 2009, Processes of carbonate precipitation in modern microbial mats: Earth Science Reviews, v. 96, p. 141-162, doi: 10.1016/j.earscirev.2008.10.005.

ENZIEN, M.V., 1990, Cyanobacteria or Rhodophyta? Interpretation of a Precambrian microfossil: Biosystems, v. 24, p. 245-251, doi: 10.1016/0303-2647(90)90039-4.

FISCHER, W.W., and KNOLL, A.H., 2009, An iron-shuttle for deep water silica in Late Archean and Early Paleoproterozoic iron formation: Geological Society of America Bulletin, v. 121, p. 222-235, doi: 10.1130/B26328.1.

GALLAGHER, K.L., KADING, T.J., BRIASSANT, O., DUPRAZ, C., and VISSCHER, P.T., 2012, Inside the alkalinity engine: the role of electron donors in the organomineralization potential of sulfate-reducing bacteria: Geobiology, v. 10, p. 518-530, doi: 10.1111/j.1472-4669.2012.00342.x.

GEITLER, L., 1930-1932, Cyanophyceae. Rabenhorst's Kryptogamen-Flora: Akademie Verlagsgesellschaft, Leipzig, Band 14, 1,196 p.

GELDSETZER, H., 1973, The tectono-sedimentary development of an algal-dominated Helikian succession on northern Baffin Island, N.W.T.: Geological Association of Canada Memoir, v. 19, p. 99-126.

GOLOVENOK, V.K., and BELOVA, N.YU., 1984, Riphean microbiotas in cherts of the Billyakh Group on the Anabar Uplift: Paleontogical Journal (English version), v. 4, p. 20-30.

GOLUBIC, S., and HOFMANN, H.J., 1976, Comparisons of modern and mid-Precambrian Entophysalidaceae (Cyanophyta) in stromatolitic algal mats: cell division and degradation: Journal of Paleontology, v. 50, p. 1074-1082.

GREEN, J., KNOLL, A.H., GOLUBIC, S., and SWETT, K., 1987, Paleobiology of distinctive benthic microfossils from the Upper Proterozoic Limestone-Dolomite "Series", East Greenland: American Journal of Botany, v. 74, p. 928-940, doi: 10.2307/2443874.

GROTZINGER J. P., and JAMES, N.P., 2000, Precambrian carbonates: evolution of understanding:

SEPM Special Publication, n. 67, p. 3–19.

GROTZINGER, J.P., and KNOLL, A.H., 1999, Proterozoic stromatolites: evolutionary mileposts or environmental dipsticks? Annual Review of Earth and Planetary Science, v. 27, p. 313-358, doi: 10.1146/annurev.earth.27.1.313.

HALVERSON, G.P. HOFFMAN, P.F., SCHRAG, D.C., MALOOF, A.C., and RICE, A.H.N., 2005, Toward a Neoproterozoic composite carbon-isotope record: Geological Society of America Bulletin, v. 117, p.1181-1207, doi: 10.1130/B25630.1.

HEAMAN, L.M., LE CHEMINANT, A.N., and RAINBIRD, R.H., 1992, Nature and timing of Franklin igneous events, Canada: implications for a late Proterozoic mantle plume and the break-up of Laurentia: Earth and Planetary Science Letters, v. 109, p. 117–131, doi: 10.1016/0012-821X(92)90078-A.

HOFMANN, H. J., 1976, Precambrian microflora, Belcher Island, Canada: significance and systematic: Journal of Paleontology, v. 50, p. 1040-1073.

HOFMANN, H.J., and JACKSON, G.D., 1987, Proterozoic ministromatolites with radial-fibrous fabrics: Sedimentology, v. 34, p. 963-971, doi: 10.1111/j.1365-3091.1987.tb00586.x.

HOFMANN, H. J., and JACKSON, G. D., 1991, Shelf-facies microfossils from the Uluksan Group (Proterozoic Bylot Supergroup), Baffin Island, Canada: Journal of Paleontology, v. 65, p. 361-381.

HOFMANN, H.J., and JACKSON, G.D., 1994, Shale-facies microfossils from the Proterozoic Bylot Supergroup, Baffin Island, Canada: Journal of Paleontology, v. 68, p. S1-S39.

HORODYSKI, R, J., and DONALDSON, J.A., 1980, Microfossils from the Middle Proterozoic Dismal Lakes Group, arctic Canada: Precambrian Research, v. 11, p. 125-159, doi: 10.1016/0301-9268(80)90043-1.

HORODYSKI, R, J., and DONALDSON, J.A., 1986, Distribution and significance of microfossils in cherts of the Middle Proterozoic Dismal lakes Group, District of Mackenzie, Northwest Territories, Canada: Journal of Paleontology, v. 57, p. 271-288.

HORODYSKI, R, J., and VONDER HAAR, S., 1975, Recent calcareous stromatolites from Laguna Mormona (Baja California) Mexico: Journal of Sedimentary Petrology, v. 45, p. 894-906.

HORODYSKI, R, J., BLOESER, B., and VONDER HAAR, S., 1975, Laminated algal mats from a coastal lagoon, Laguna Mormona, Baja California, Mexico: Journal of Sedimentary Petrology, v. 47, p. 680-696.

JACKSON, G. D., and IANNELLI, T. R., 1981, Rift-related cyclic sedimentation in the Neohelikian Borden Basin, northern Baffin Island: Geological Survey of Canada Paper 81-10, p. 269-302.

JACKSON, G. D. and MORGAN, W. C., 1975, Geology of the Pond Inlet map-area, Baffin Island, District of Franklin: Geological Survey of Canada Paper 74-25, 33 p.

JACKSON, G. D., KNIGHT, R. D. and LEBEL, D., 1985, Neohelikian Bylot Supergroup of Borden Rift basin, northwestern Baffin Island, District of Franklin: Geological Survey of Canada Paper 85-1A, p. 639-649.

KAH, L.C., 1997, Sedimentological, geochemical, and paleobiological interactions on a Mesoproterozoic carbonate platform: Society Cliffs Formation, northern Baffin Island, Arctic Canada. Ph.D. thesis, Harvard University, Cambridge, Massachusetts.

KAH, L. C., 2000, Depositional $\delta^{18}O$ signatures in Proterozoic dolostones: constraints on seawater chemistry and early diagenesis: SEPM Special Publication, n. 67, p. 345-360.

KAH, L. C., and BARTLEY, J.K., 2011. The Precambrian record of evolving oxygen: International Geology Review, v. 53, p. 1424-1442, doi: 10.1080/00206814.2010.527651.

KAH, L. C., and KNOLL, A. H., 1996, Microbenthic distribution of Proterozoic tidal flats: environmental and taphonomic considerations: Geology, v. 24, p. 79-82, doi: 10.1130/0091-7613(1996)024<0079:MDOPTF>2.3.CO;2.

KAH, L.C., and RIDING, R. 2007. Mesoproterozoic carbon dioxide levels inferred from calcified cyanobacteria: Geology, v. 35, p. 799–802, doi: 10.1130/G23690A.1.

KAH, L. C., BARTLEY, J. K., and TEAL, D. A., 2012. Chemostratigraphy of the Late Mesoproterozoic Atar Group, Taoudeni Basin, Mauritania: Muted isotopic variability, facies correlation, and global isotopic trends: Precambrian Research, v. 200-203, p. 82-103, doi: 10.1016/j.precamres.2012.01.011.

KAH, L. C., LYONS, T. M., and CHELSEY, J. T., 2001, Geochemistry of a 1.2 Ga carbonate-evaporite succession, northern Baffin and Bylot Islands: implication for Mesoproterozoic marine evolution: Precambrian Research, v. 111, p. 203-234, doi: 10.1016/S0301-9268(01)00161-9.

KAH, L. C., SHERMAN, A. G., NARBONNE, G. M., KNOLL, A. H., and KAUFMAN, A. J., 1999, $\delta^{13}C$ stratigraphy of the Proterozoic Bylot Supergroup, Baffin Island: implications for regional stratigraphic correlations: Canadian Journal of Earth Sciences, v. 36, p. 313-332, doi: 10.1139/cjes-36-3-313.

KNOLL, A.H., and GOLUBIC, S., 1979, Anatomy and taphonomy of a Precambrian algal stromatolite: Precambrian Research, v. 10, p. 115-151, doi: 10.1016/0301-9268(79)90022-6.

KNOLL, A.H., and SEMIKHATOV, M.A., 1998, The genesis and time distribution of two distinctive Proterozoic stromatolite microstructures: Palaios, v. 13, p. 407-421, doi: 10.2307/3515471.

KNOLL, A. H., and SERGEEV, V.N., 1995, Taphonomic and evolutionary changes across the Mesoproterozoic-Neoproterozoic transition: Neues Jahrbuch für Geologie und Paläontologie Abhandlungen, v. 195, p. 289-302.

KNOLL, A.H., and SWETT, K., 1990, Carbonate deposition during the late Proterozoic era: An example from Spitsbergen: American Journal of Science, v. 290-A, p. 104-132.

KNOLL, A.H., HAYES, J.M., KAUFMAN, A.J., SWETT, K., and LAMBERT, I., 1986, Secular variation in carbon isotope ratios from Upper Proterozoic successions of Svalbard and East Greenland: Nature, v. 321, p. 832-838, doiI: 10.1038/321832a0.

KNOLL, A. H., SWETT, K., and MARK, J., 1991, Paleobiology of Neoproterozoic tidal flat/lagoonal complex: the Draken Conglomerate Formation, Spitsbergen, Journal of Paleontology, 65(4), p. 531-570.

LE CHEMINANT, A. N., and HEAMAN, L. M., 1989, Mackenzie igneous events, Canada: Middle Proterozoic hotspot magmatism associated with ocean opening: Earth and Planetary Science Letters, v. 96, p. 38-48, doi: 10.1016/0012-821X(89)90122-2.

LEMON, R.H.H., and BLACKADAR, R.G., 1963, Admirality Inlet area, Baffin Island, District of Franklin: Geological Survey of Canada, Memoir 328.

MALIVA, R.G., MISSIMER, T.M., LEO, K.C., STATOM, R.A., DUPRAZ, C., LYNN, M., and DICKSON, J.A.D., 2000, Unusual calcite stromatolites and pisoids from a landfill leachate collection system: Geology, v. 28, pp. 931-934, doi: 10.1130/0091-7613(2000)28<931:UCSAPF>2.0.CO;2.

MATA, S. A., HARWOOD, C. L., CORSETTI, F. A., STORK, N. J., EILERS, K., BERELSON, W. M., and SEAR, J. R., 2012, Influence of gas production and filament orientation on stromatolite microfabric: Palaios, v. 27, p. 206-219, doi: 10.2110/palo.2011.p11-088r.

MERZ, M.U., 1992, The biology of carbonate precipitation by cyanobacteria. Facies, v.26, p. 81-102.

MONTY, C.L.V., 1976, The origin and development of cryptalgal fabrics, *in* Walter, M.R., ed., Stromatolites: New, York: Elsevier, p. 193-249.

MUIR, M.D., 1976, Proterozoic microfossils from the Amelia Dolomite, McArthur Basin, Northern Territory: Alcheringa, v. 1, p. 143-158.

NYBERG, A.V., and SCHOPF, J.W., 1984, Microfossils in stromatolitic cherts from the upper Proterozoic Min'Yar Formation, southern Ural Mountains, USSR: Journal of Paleontology, v. 58, p. 738-772.

OEHLER, J.H., 1977, Precambrian microfossils and associated mineralization in the McArthur deposit, Northern Territory, Australia: Alcheringa, v. 1, p. 315-349.

PEHRSSON, S.J., and BUCHAN, K.L., 1999, Borden dykes of Baffin Island, NWT: A Franklin U-Pb Baddeleyite age and a paleomagnetic interpretation: Canadian Journal of Earth Sciences, v. 36, p. 65-73, doi: 10.2110/palo.2011.p11-088r.

PENTECOST, A., and RIDING, R., 1986, Calcification in cyanobacteria, *in* Leadbeater, B.S.C., and Riding, R., eds., Biomineralization in Lower Plants and Animals: Systematics Association Special Volume 30: Oxford, Clarendon Press, p. 73–90.

POLLOCK, M.D., KAH, L.C., AND BARTLEY, J.K., 2006, Morphology of molar-tooth structures in Precambrian carbonates: influence of substrate rheology and implications for genesis: Journal of Sedimentary Research, v. 76, p. 310-323, doi: 10.2110/jsr.2006.021.

SAMUELSSON, J., DAWES, P.R., AND VIDAL, G., 1999, Organic-walled microfossils from the Proterozoic Thule Supergroup, Northwest Greenland: Precambrian Research, v. 96, p. 1-23, doi: 10.1016/S0301-9268(98)00123-5.

SCHOPF, J.W., 1968, Microflora of the Bitter Springs Formation, Late Precambrian central Australia: Journal of Paleontology, v. 42, p. 651-688.

SEREBRYAKOV, S.N., 1976, Biotic and abiotic factors controlling the morphology of Riphean stromatolites, *in* Walter, M.R., ed., Stromatolites: New York: Elsevier, p. 321-336.

SEMIKHATOV, M.A., GEBELEIN, C.D., CLOUD, P., AWRAMIK, S.M., and BENMORE, W.C., 1979, Stromatolite morphogenesis – progress and problems: Canadian Journal of Earth Sciences, v. 19, p. 992-1015.

SERGEEV, V.N., 1994, Microfossils in cherts from the Middle Riphean (Mesoproterozoic) Avzyan Formation, southern Ural Mountains, Russian Federation: Precambrian Research, v. 65, p. 231-254, doi: 10.1016/0301-9268(94)90107-4.

SERGEEV, V.N., KNOLL, A.H., and GROTZINGER, J.P., 1995, Paleobiology of the Mesoproterozoic Billyakh Group, northern Siberia: Paleontological Society Memoir 39, p.1-37.

STROTHER, P. K., KNOLL, A. H. and BARGHOORN, E. S., 1983, Micro-organisms from the late Precambiran Narssârssuk Formation, north-western Greenland: Palaeontology, v. 26, p. 1-32.

SUMNER, D.Y., 1997, Late Archean calcite-microbe interactions: Two morphologically distinct microbial communities that affected calcite nucleation differently: Palaios, v. 12, p. 302-318, doi: 10.2307/3515333.

TURNER, E., 2009, Mesoproterozoic carbonate systems in the Borden Basin, Nunavut: Canadian Journal of Earth Sciences, v. 46, p. 915-938, doi: 10.1139/E09-062.

WALTER, M.R., 1992, Proterozoic Stromatolites. in Schopf, J.W., and Klein, C., eds., The Proterozoic Biosphere: A Multidisciplinary Study: New York, Cambridge, p. 253-260.

WALTER, M.R., KRYLOV, I.N. and MUIR, M.D., 1988, Stromatolites from Middle and Late

Proterozoic sequences in the McArthur and Georgina Basins and the Mount Isa Province, Australia: Alcheringa, v. 12, p. 79-106.

ZHANG, Y., 1981, Proterozoic stromatolitic microfloras of the Gaoyuzhuang Formation (Early Sinian, Riphean), Hebei, China: Journal of Paleontology. v. 55, p. 485-506.

FIGURE CAPTIONS

FIGURE 1 – Geologic map of the Milne Inlet region, Baffin Island, showing location and distribution of stratigraphic units within the Bylot Supergroup. Samples (black circles) tied to measured sections at Mala River (MR), Tremblay Sound (TS), Milne Inlet (MI), and White Bay (WB).

FIGURE 2 – Populations of *Siphonophycus inornatum* and *S. capitaneum* in filament-dominated mat facies. A-D show variously oriented silicified populations (A: G4, G53/0; B: G4, J53/0, C: G4, L51/2; D: DAC-10, J38/4). E) Molds of *S. capitaneum* sheaths preserved in carbonate (DAC-10, S62/4). Bar in E = 250 μm for A, D and E, = 800 μm for B, and = 500 μm for C.

FIGURE 3 – Microfossils and fabrics in filament-dominated mat facies. A) *Siphonophycus inornatum* (G23, N49/1). B) Mat fabric of laminated EPS, with no well preserved microfossils. C) Mat building assemblage of *Siphonophycus inornatum* and larger *S. capitaneum* (DAC-5, N70/3). D *Eomicrocoleus crassus* (G4, B54/3). E) Cross section of *E. crassus*, showing evidence of multiple trichomes (DAC-5, E53/0). F) *Mycoccoides* sp. 2 (DAC-28, M50/0). Bar in F = 30 μm for A, = 1 mm for B, = 100 μm for C, = 30 μm for D, = 70 μm for E, and = 60 μm for F.

FIGURE 4 – Microfossils in Angmaat cherts. A) Endolithic cyanobacteria penetrating lamina in laminated precipitate-coccoidal mat facies (34, N48/4). B) *Eoentphysalis belcherensis* colony in coccoidal mat layer (DAS 26, N65/4). C) *Siphonophycus robustum* in thin filament mat (34,

F55/2). D and E) *Sphaerophycus parvum* dyads within the filament-dominated mat community (D: G25, M43/1; E: G25, L41/4). F) Unnamed multilamellate spheroid with opening, possibly related to *Polybessurus*, in filament-dominated mat (thin section G4, Efc G57/2). G) *Gloeodiniopsis magna* (thin section 35, Efc V41/2). H) Unnamed spheroids with tubular extensions (G25, Efc). I-L) *Gloeodiniopsis lamellose* (I: G25, M43/4; J: 35, T48/1; K: G4, E59/0, L: DAC-5, H53/0). Bar in G = 100 μm for A, = 150 μm for B, = 30 μm for C, = 10 μm for D, E, and L, = 15 μm for F, I, J, and K, = 20 μm for G, and = 25 μm for H.

FIGURE 5 – Mat dwelling populations in filament-dominated mats. A and B) *Polybessurus bipartitus* (A: G4, P57/0; B: G4, K61/1). C and D) *Sphaerophycus medium* (C: G25, M43/0; D: G25, M43/2) E. *Gloeocapsa magna* (34, 46/2). F. *Myxococcoides* sp. 1 (G4, O56/0). Bar in F = 60 μm for A and B, = 10 μm for C and D, and = 20 μm for E and F.

FIGURE 6 – Additional Angmaat fossils. A-C) *Eogloeocapsa bella* (A: DAC-5, O67/3; B: DAC-5, V68/0; C: DAC-5, W63/2). D and E) *Bangiomorpha pubescens* (35, F54/3). Bar in E = 50 μm for A, B and D, = 20 μm for C, and = 70 μm for E.

FIGURE 7 – Crystal fan-dominated precipitate facies (all illustrated specimens are reposited in Harvard University Paleobotanical Collection 64840; thin section – G12 in this case – and, for microfossils, England finder coordinates are given in parentheses). A) Overview showing silicified region (brown) above diagenetically altered carbonates. B, C, and F) Fine acicular microfabrics reflecting original carbonate precipitates, preserved by early diagenetic silicification; note dissolution voids in B and zonation in B, C and F, reflecting variations in the

incorporation of organic matter during crystal growth. D) Possible microfossils (endolithic cyanobacteria?) oriented parallel to crystal growth axes. E) Originally aragonitic crystals, with square terminations. Scale bar in D = 0.75 mm in A; = 250 μm in B, C, and F; = 2 μm in D; and = 200 μm in E.

FIGURE 8 – Field views of thin filament-tufted mat facies. A) Tufted mats draped by white micrite in lower part and partially silicified tufts in upper part of image; black zone of pole = 10 cm. B) Silicified tufts – black chert marks organic–rich tufts of filaments, whereas white chert is predominantly original void space preserved by early mineralization; note pen for scale.

FIGURE 9 – Thin filament-tufted mats in thin section (G11). A) Silicified (above) and unsilicified fabrics. B and C, Higher resolution views of silificied mat fabric, showing oriented thin filamentous microfossils and primary void spaces, some originally filled with fans of precipitated carbonate (arrow in C). Bar in A = 4.5 mm for A, and = 400 μm in B and C.

FIGURE 10 – Laminated precipitates and coccoid-rich mat facies (G13). A) Interspersed silicified and unsilicified lithologies, showing characteristic fabric development. B) Higher resolution image showing stacked, organic-rich mat layers preserved in chert. C) Higher resolution image showing layered precipitates preserved in chert. Bar in C = 5 mm in A, = 400 μm in B, and 175 μm in C.

FIGURE 11 – A) Interlaminated thin filament mats (TFM) with abundant primary void space and laminated precipitate/coccoidal mats (LP/CM) that display few if any primary voids.

Carbonate microspar preserved within many voids in black cherts (34). B) Vertical tuft of filamentous microfossils, outlining void space (noted by arrow in A; 34, K53/2). Bar in B = 3.5 mm in A, and = 15 μm in B.

FIGURE 12 – Filament-dominated mat facies (A: DAC-10 and B: G4). Note arenitic carbonate beneath mat accumulation in A.

FIGURE 13 – Thin section DAC-5, showing interlayering of filamentous mats built by *Siphonophycus inornatum*, thin filament-mats, an *Eogloeocapsa* accumulation, and a thin grainstone; note position of *Bangiomorpha* within the *S. inornatum* mat interval. Bar = 5 mm.

FIGURE 14 – Diagram showing the distribution of microfossil taxa, seafloor precipitates, preserved gas bubbles, and dissolution features among the five microfacies recognized in Angmaat samples. Thicker lines indicate principal mat builders, as inferred from the density and orientation of microfossils within these populations. Thinner lines indicate populations that lived in mats but did not play a major role in their construction.

FIGURE 15 -- Distinctive mat petrofabrics comparable to those of the Angmaat Formation preserved in cherts within mid-Proterozoic carbonate accumulations from northwestern Greenland (A), Siberia (B,D, and F), China (C) and Australia (E). Bar in A = 5 mm for A and C, = 1 cm for B, and = 100 μm for D-F.

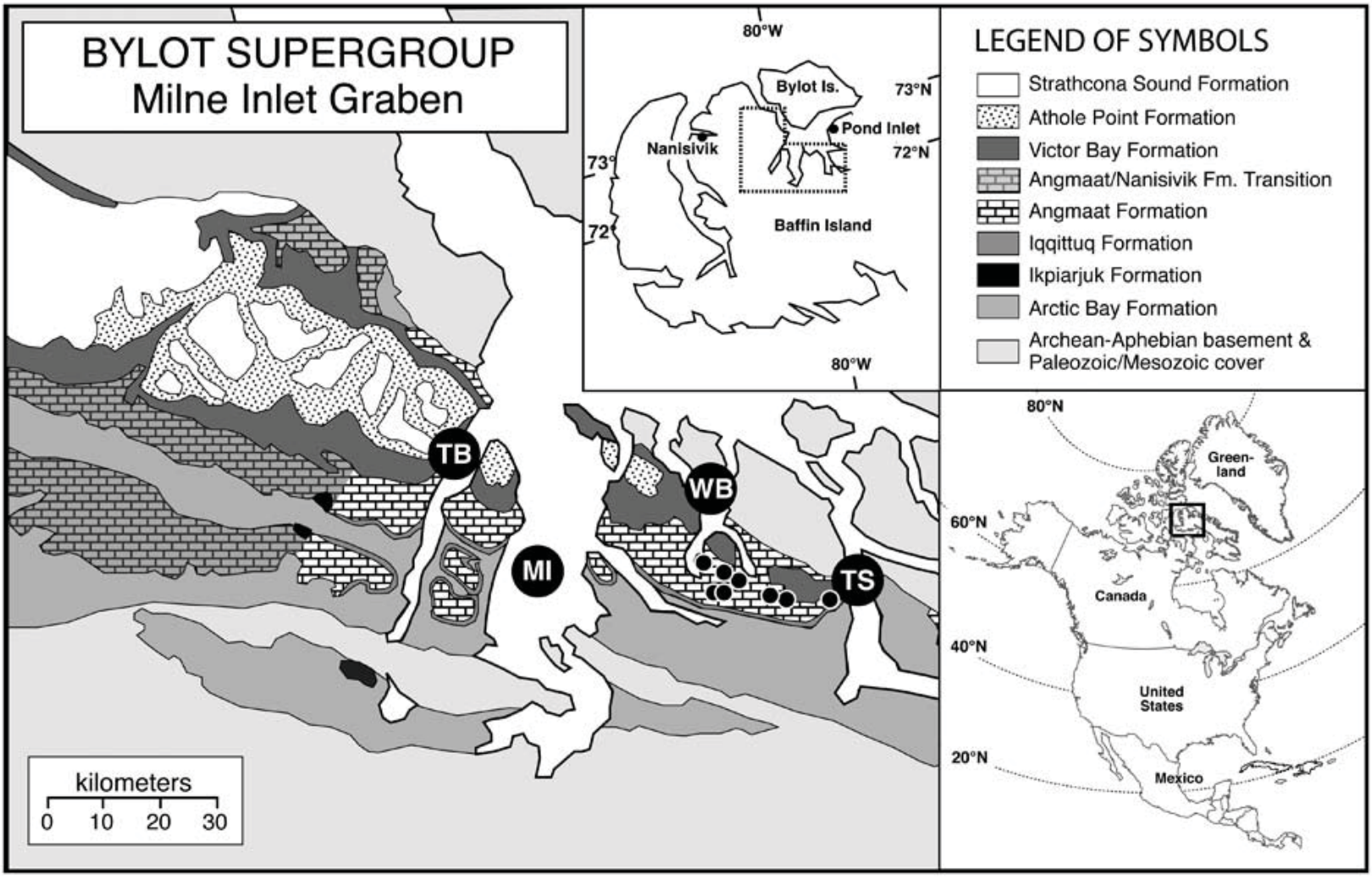
BYLOT SUPERGROUP
Milne Inlet Graben
80°W
Bylot Is.
73°N
Pond Inlet
72°N
Nanisivik
73°
72°
Baffin Island
80°W
LEGEND OF SYMBOLS
Strathcona Sound Formation
Athole Point Formation
Victor Bay Formation
Angmaat/Nanisivik Fm. Transition
Angmaat Formation
Iqqittuq Formation
Ikpiarjuk Formation
Arctic Bay Formation
Archean-Aphebian basement & Paleozoic/Mesozoic cover
TB
WB
MI
TS
kilometers
0 10 20 30
80°N
Green-land
60°N
Canada
40°N
United States
20°N
Mexico

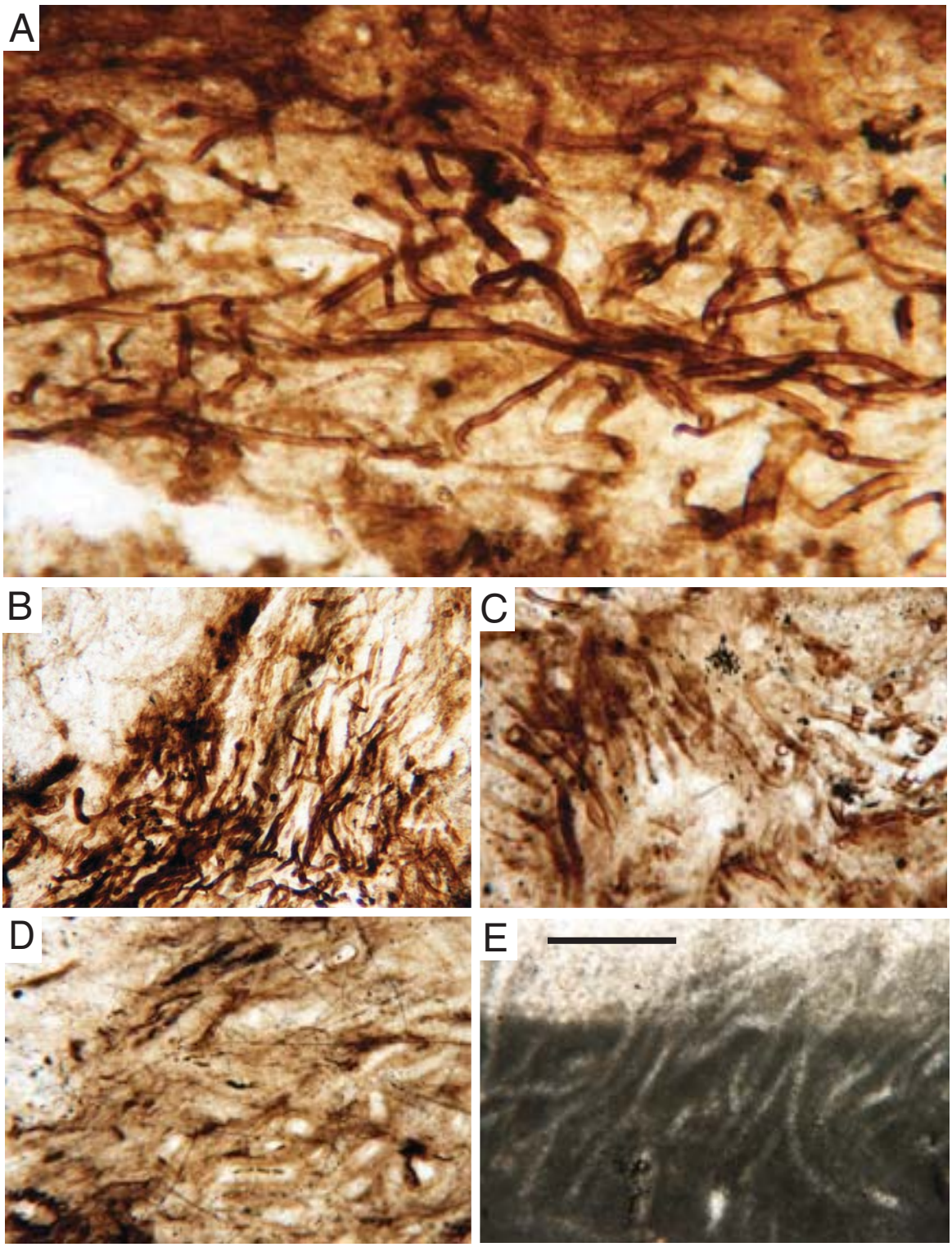
A
B
C
D
E

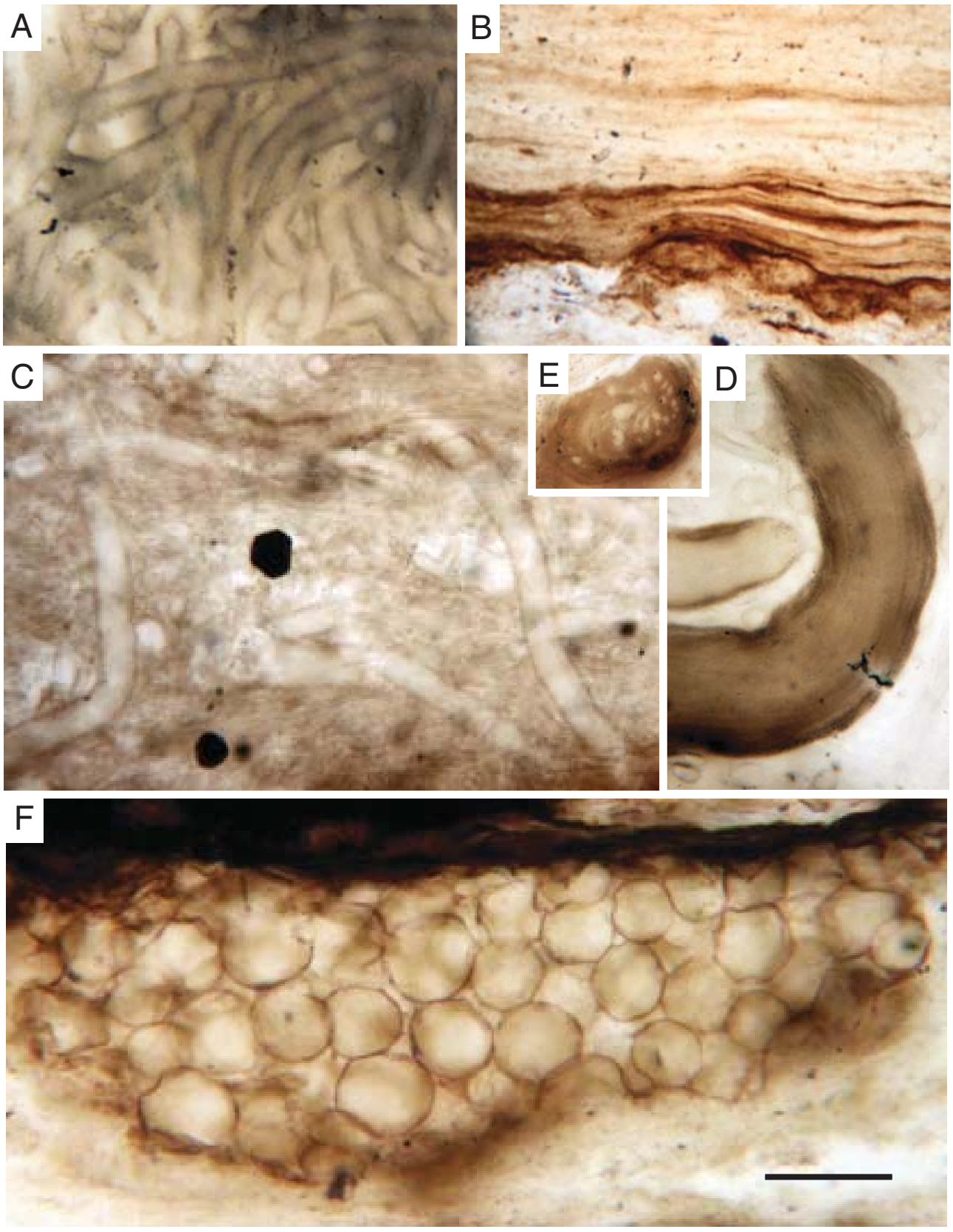
A
B
C
E
D
F

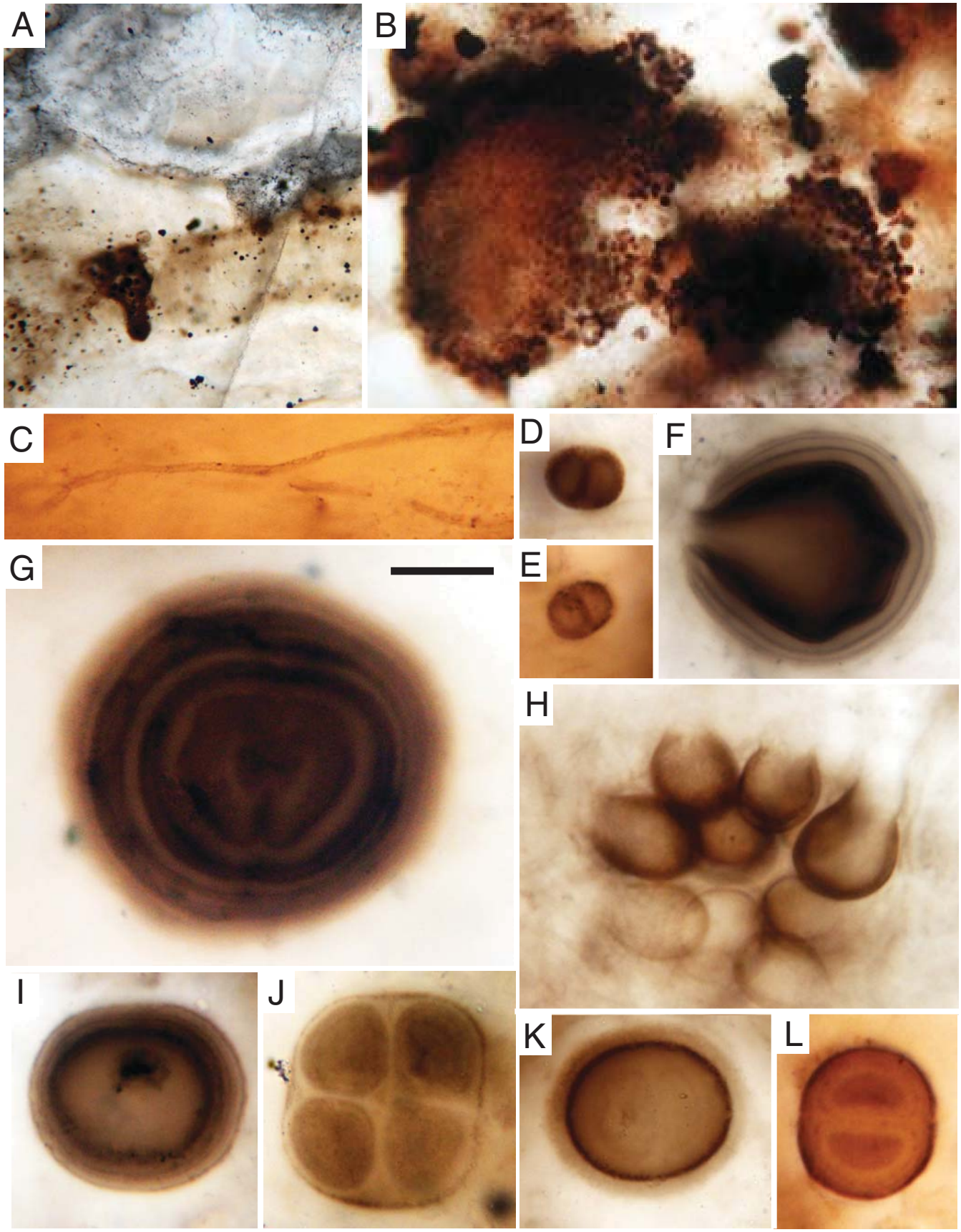
A
B
C
D
F
G
E
H
I
J
K
L

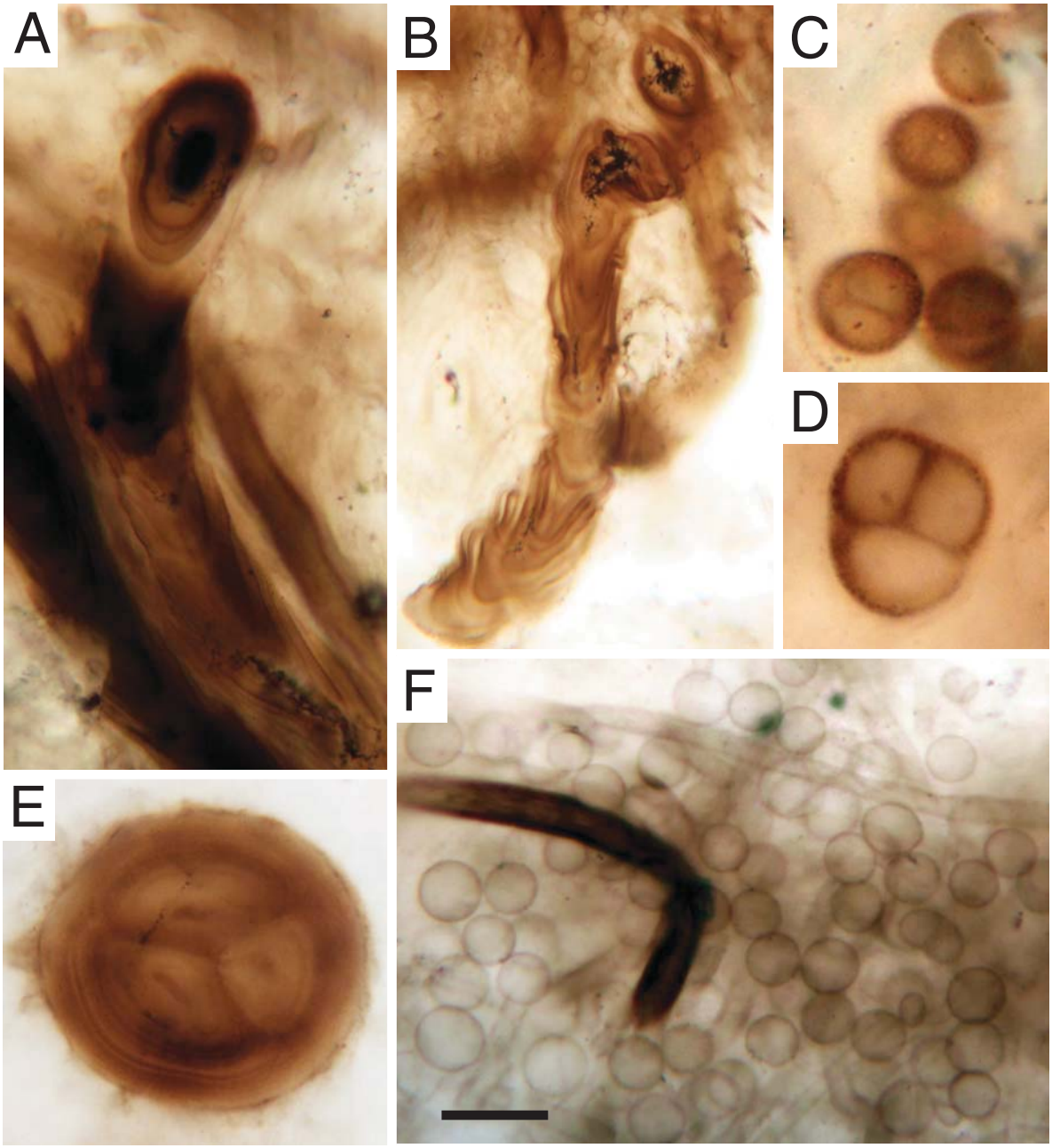
A
B
C
D
E
F

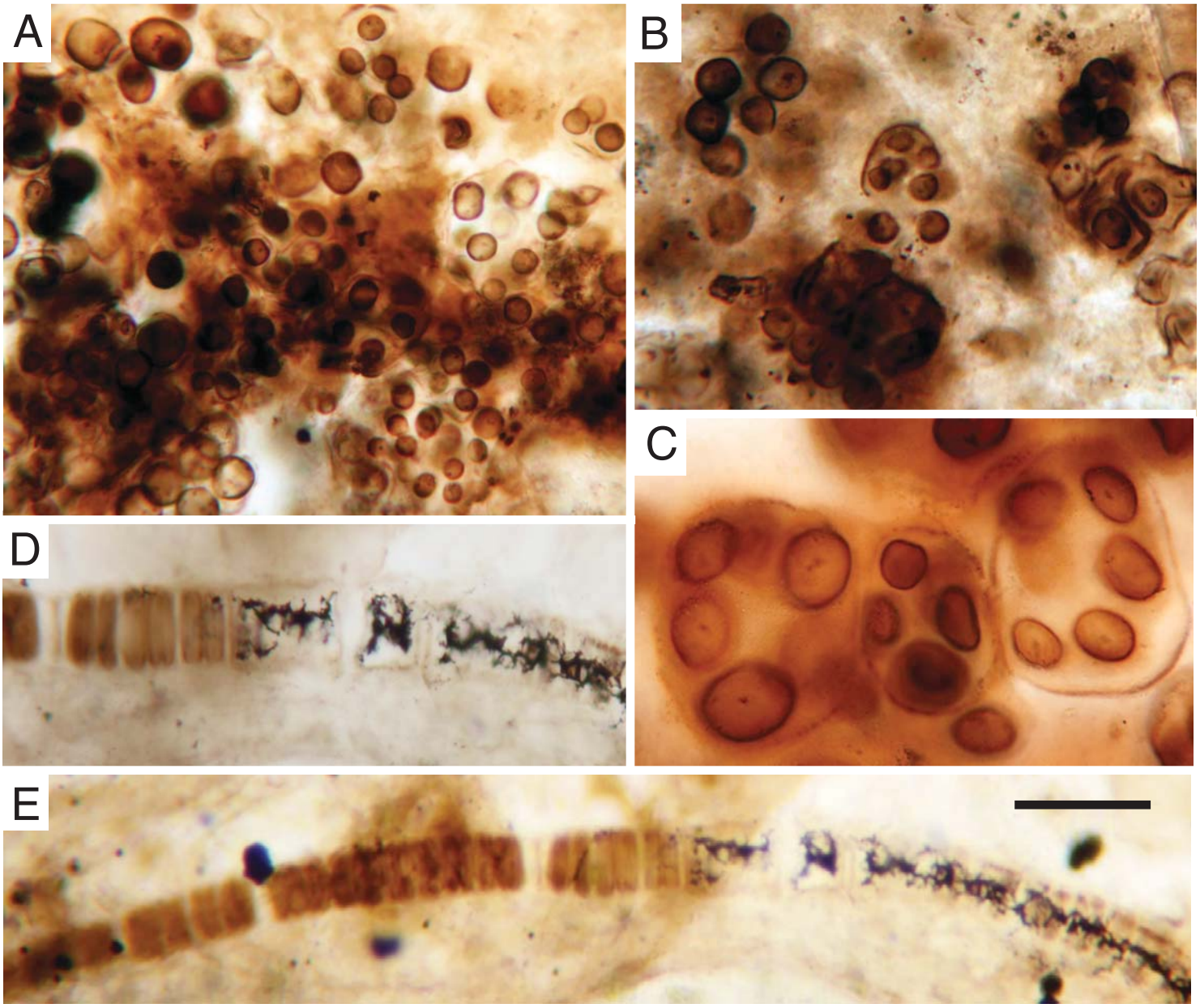
A
B
C
D
E

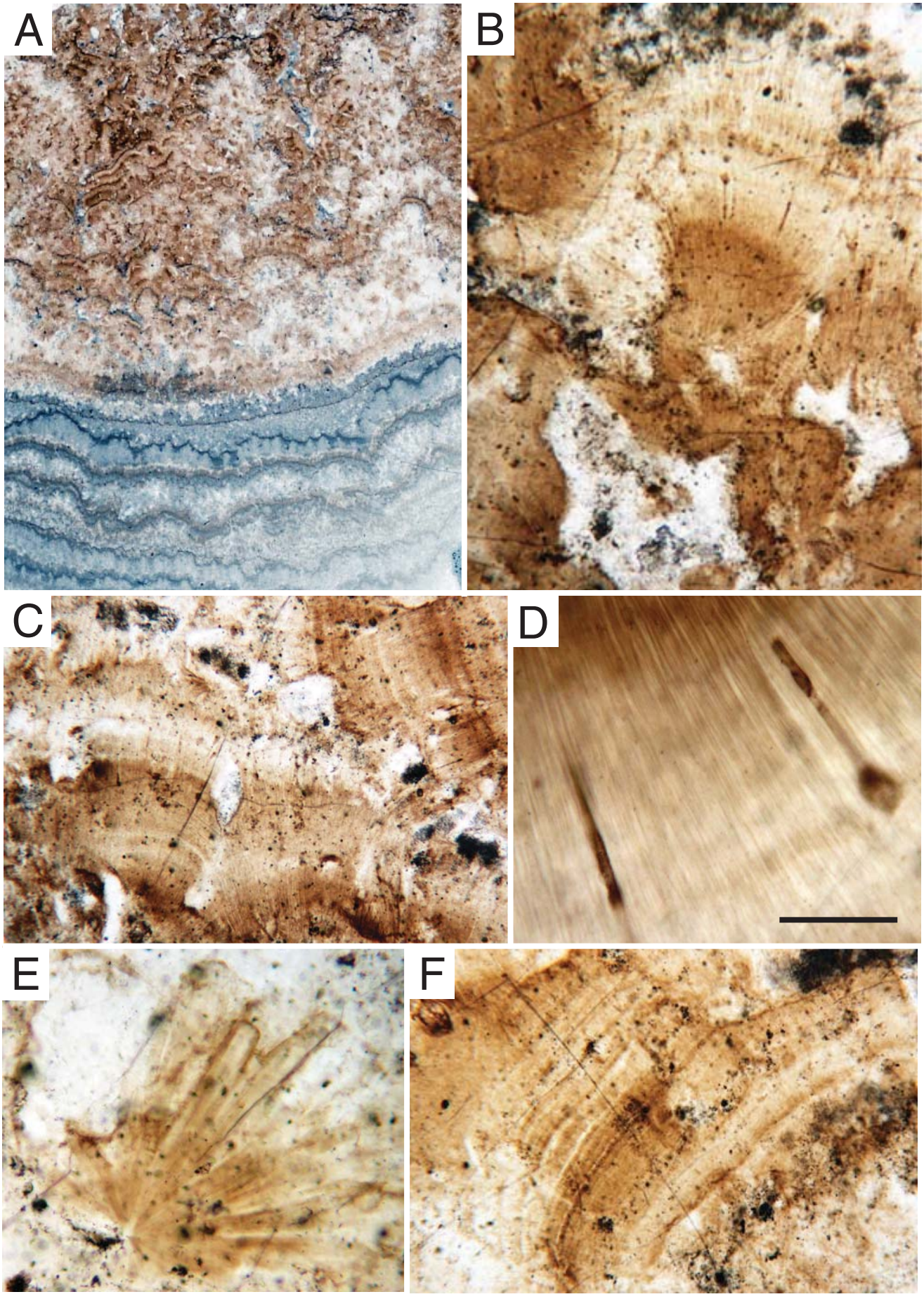
A
B
C
D
E
F

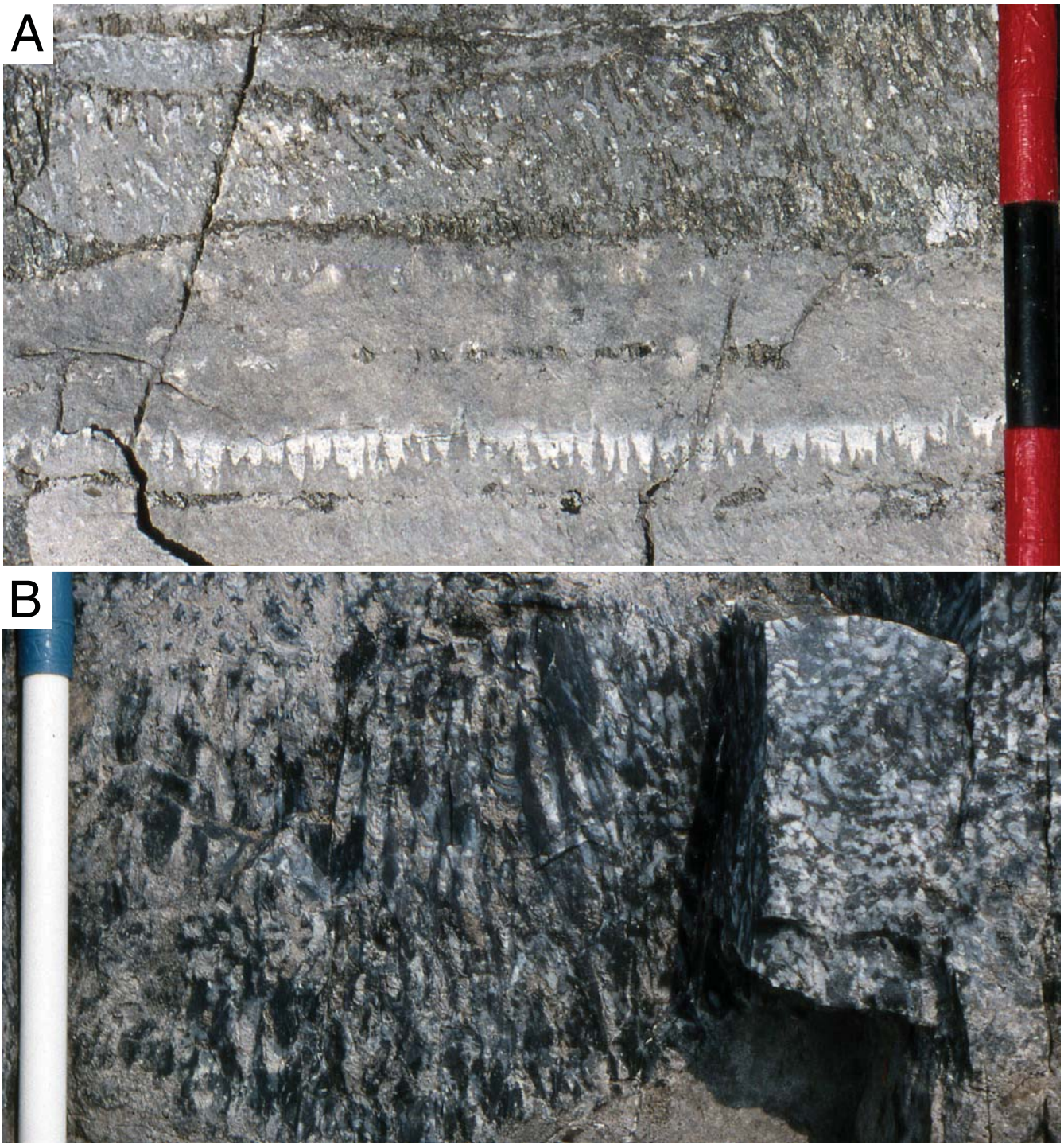
A
B

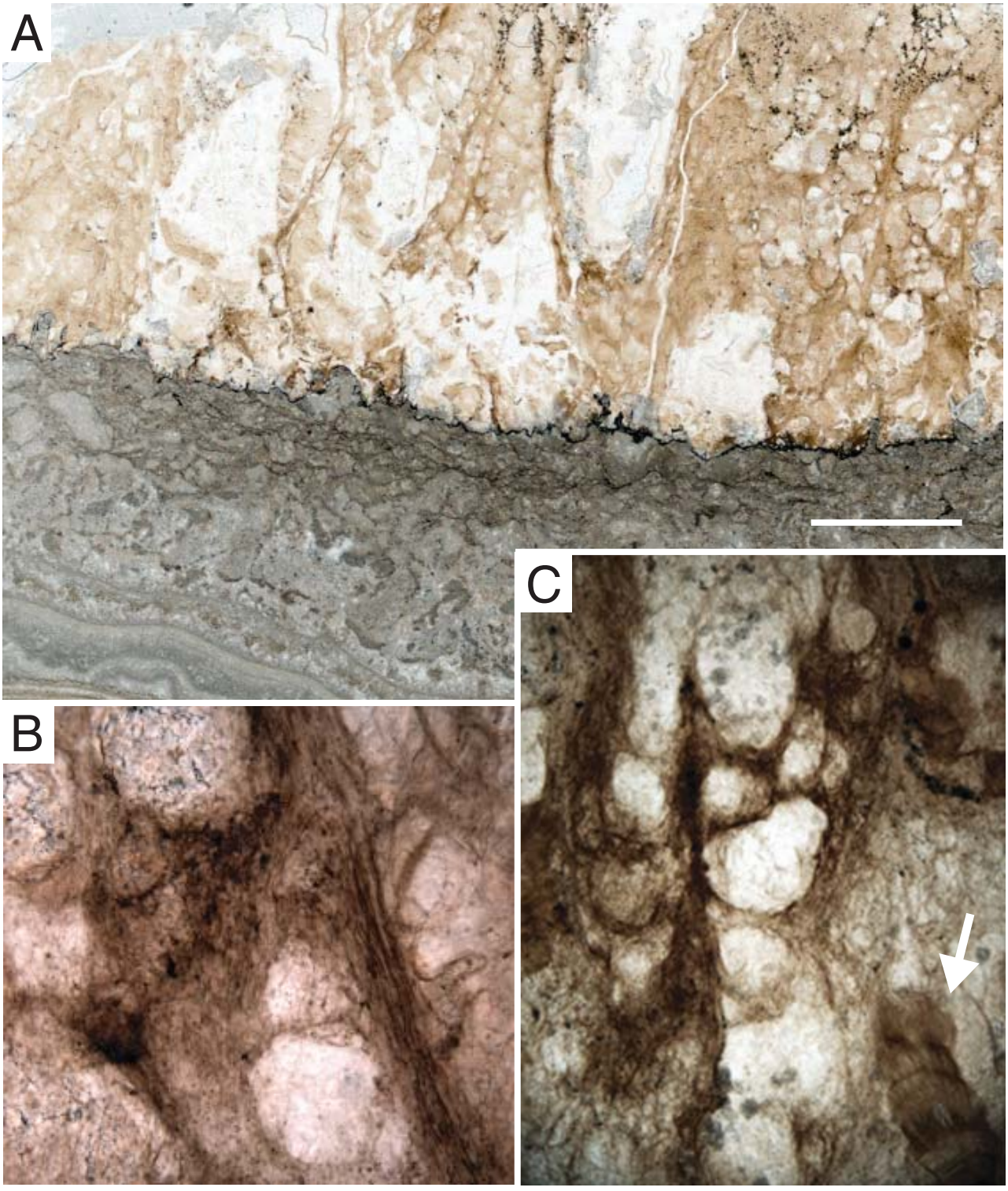
A
B
C

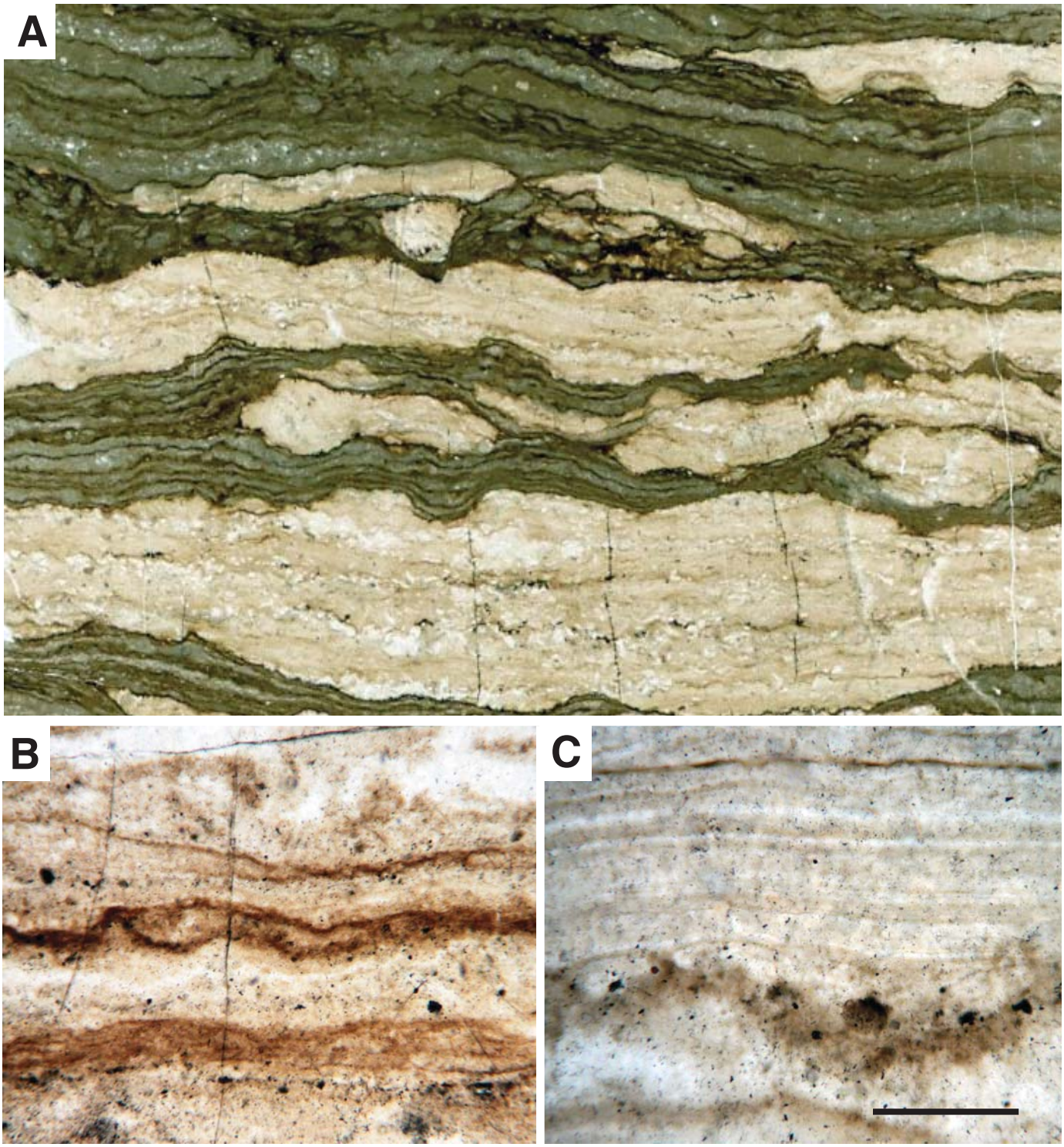
A
B
C

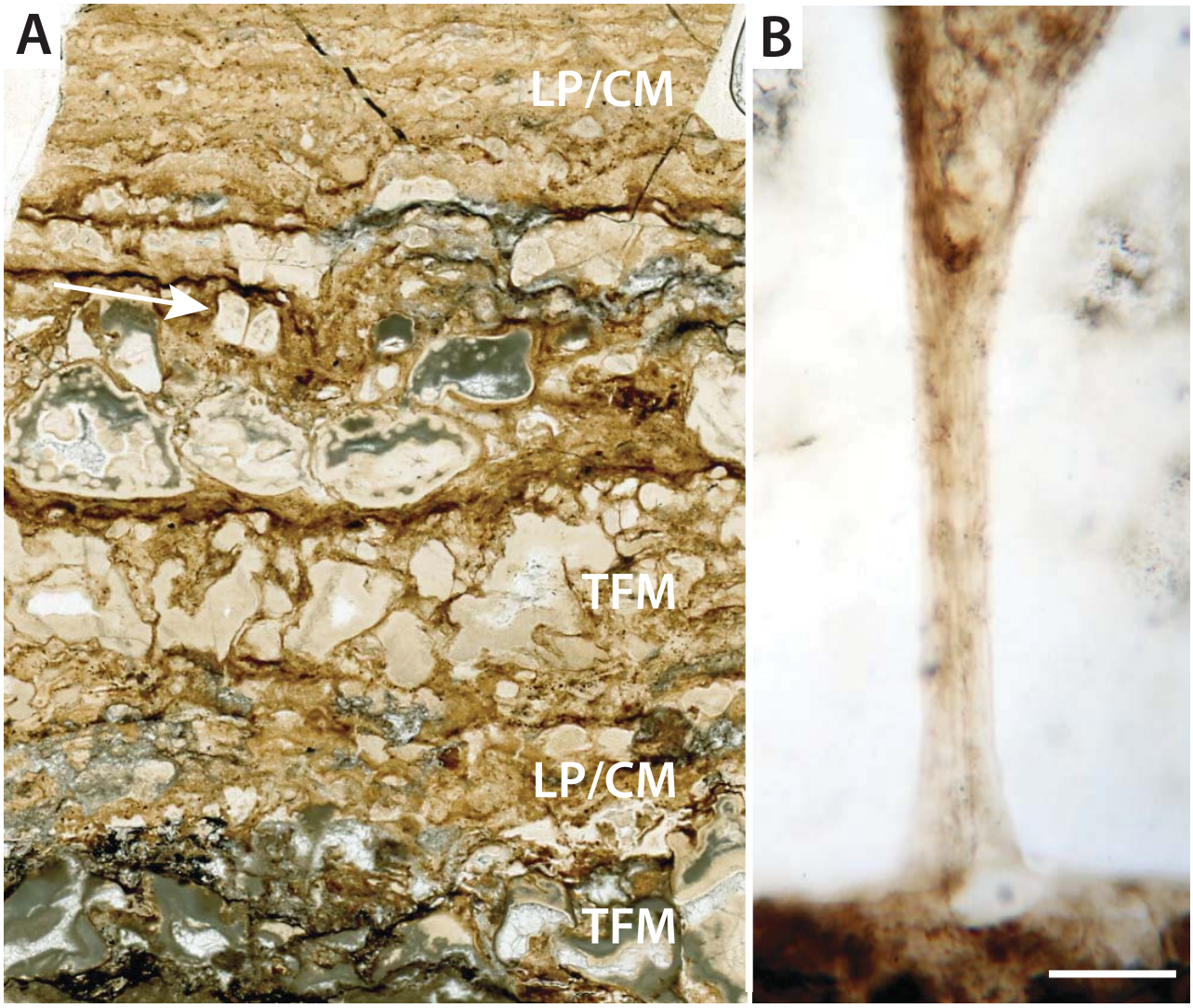
A
LP/CM
TFM
LP/CM
TFM
B

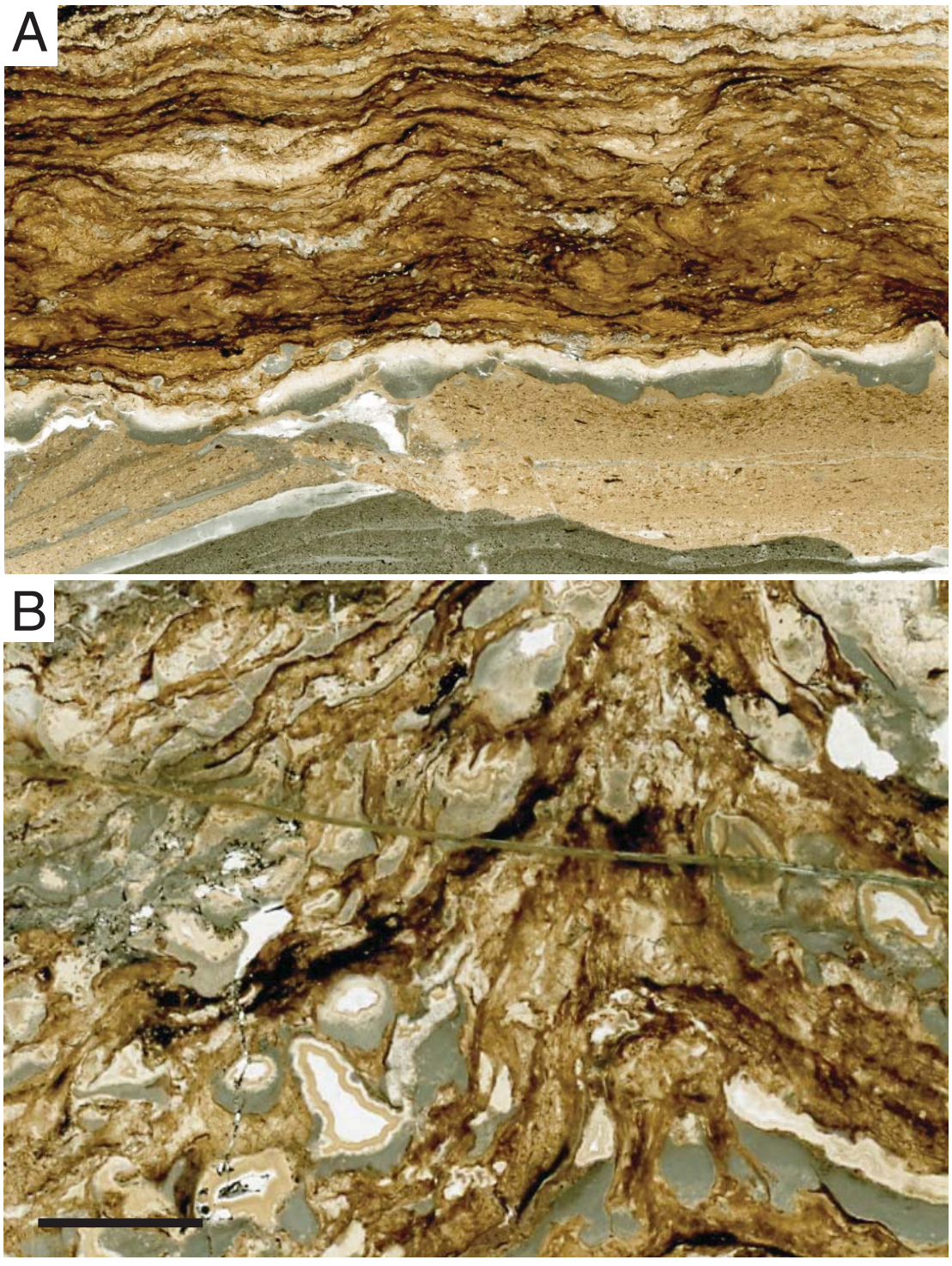
A
B

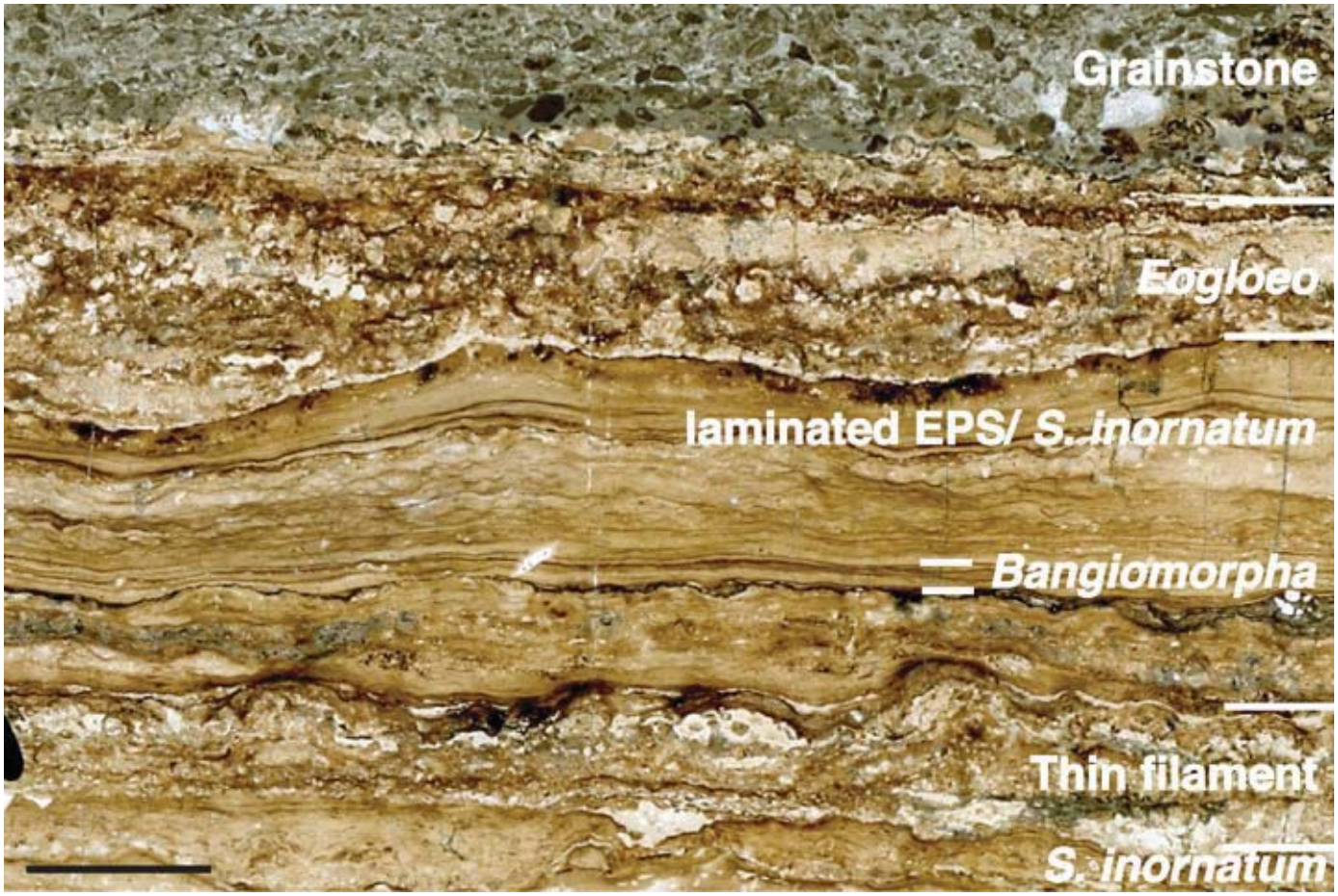
Grainstone
Eogloeo
laminated EPS/ S. inornatum
Bangiomorpha
Thin filament
S. inornatum

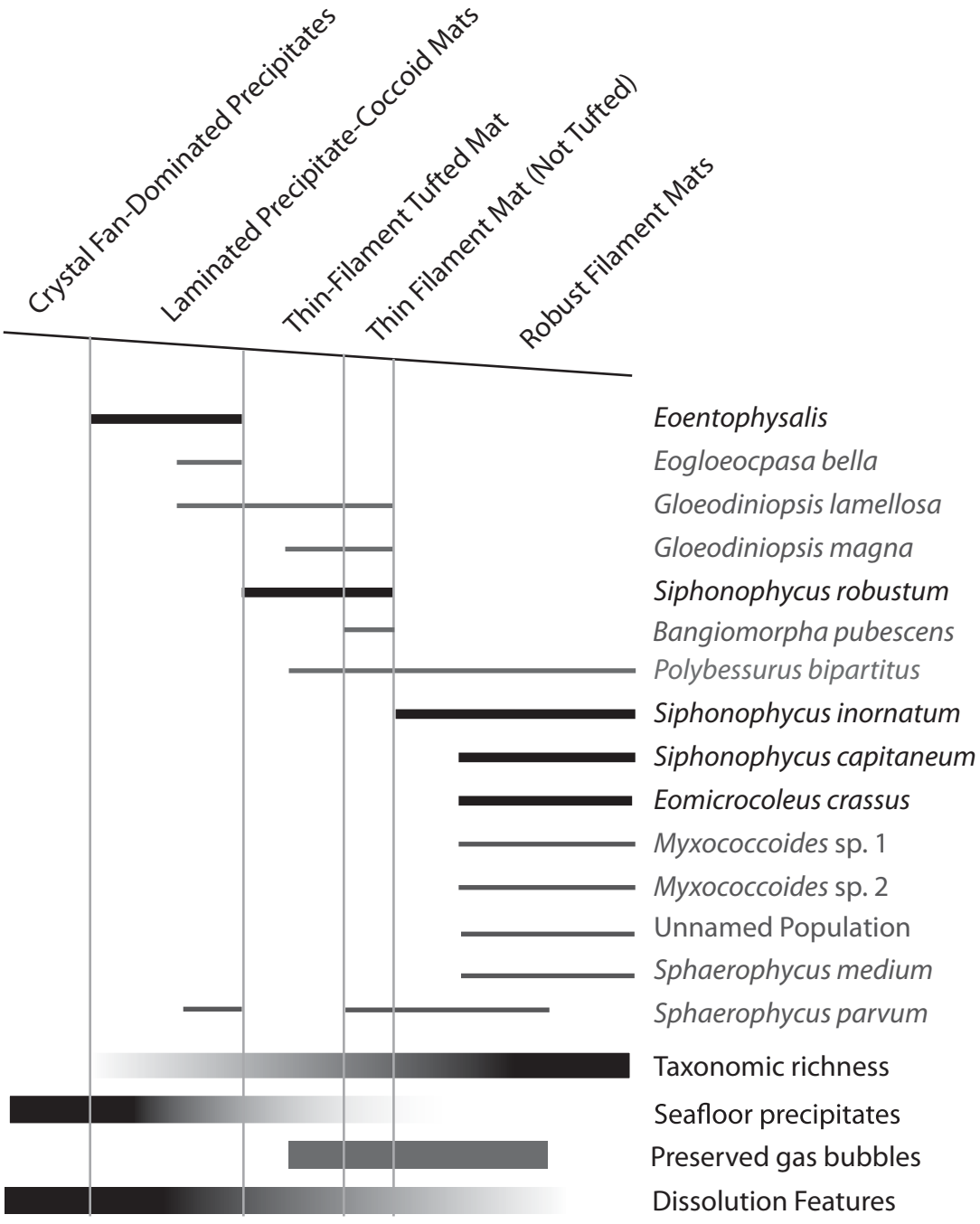
Crystal Fan-Dominated Precipitates
Laminated Precipitate-Coccoid Mats
Thin-Filament Tufted Mat
Thin Filament Mat (Not Tufted)
Robust Filament Mats
Eoentophysalis
Eogloeocpasa bella
Gloeodiniopsis lamellosa
Gloeodiniopsis magna
Siphonophycus robustum
Bangiomorpha pubescens
Polybessurus bipartitus
Siphonophycus inornatum
Siphonophycus capitaneum
Eomicrocoleus crassus
Myxococcoides sp. 1
Myxococcoides sp. 2
Unnamed Population
Sphaerophycus medium
Sphaerophycus parvum
Taxonomic richness
Seafloor precipitates
Preserved gas bubbles
Dissolution Features

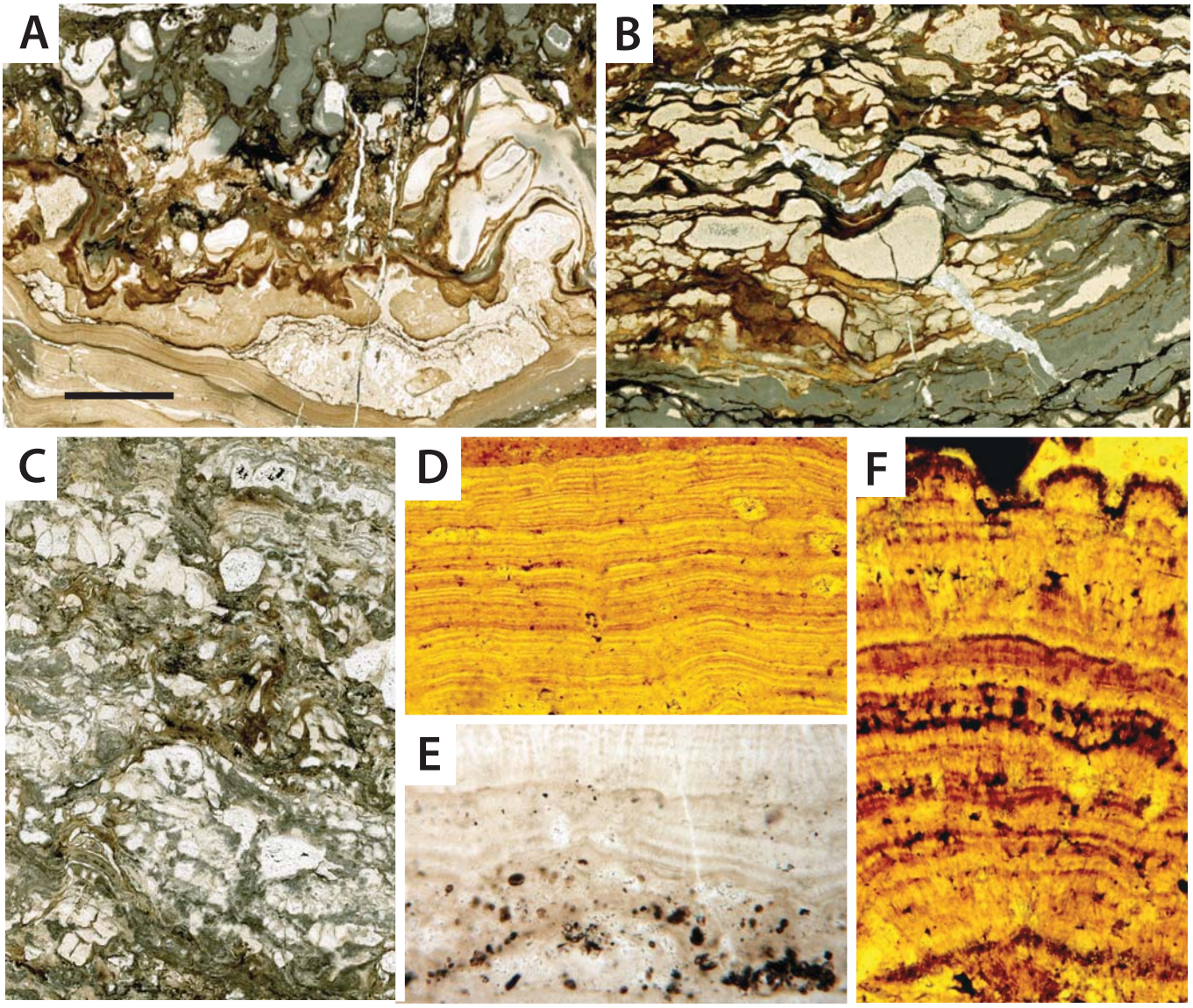
A
B
C
D
E
F